Short title: Hydraulic failure and repair in grapevine

Correspondence to: Dr. Guillaume Charrier

e-mail: guillaume.charrier@bordeaux.inra.fr

Phone: +33 5 40 00 36 64

Address: UMR 1202 Biodiversité Gènes & Communautés INRA/Université Bordeaux, Bâtiment B2 - allée G. St Hilaire, CS 50023, 33615 Pessac Cedex – France

Evidence for hydraulic vulnerability segmentation and lack of xylem refilling under tension

Charrier G[1,2]*, Torres-Ruiz JM[2], Badel E[3], Burlett R[2], Choat B[4], Cochard H[3], Delmas CEL[5], Domec JC[6,7], Jansen S[8], King A[9], Lenoir N[10], Martin-StPaul N[11], Gambetta GA[1], Delzon S[2]

[1]Bordeaux Science Agro, Institut des Sciences de la Vigne et du Vin, Ecophysiologie et Génomique Fonctionnelle de la Vigne, UMR 1287, F– 33140 Villenave d'Ornon, France
[2] BIOGECO, INRA, Univ. Bordeaux, 33610 Cestas, France
[3] PIAF, INRA, UCA, 63000 Clermont-Ferrand, France
[4] Hawkesbury Institute for the Environment, University of Western Sydney, Richmond, NSW 2753, Australia
[5] UMR SAVE, INRA, BSA, Univ. Bordeaux, 33882, Villenave d'Ornon, France
[6] Bordeaux Science Agro, UMR 1391 ISPA, F-33882 Villenave d'Ornon, France
[7] Nicholas School of the Environment, Duke University, Durham, North Carolina 27708, USA
[8] Institute for Systematic Botany and Ecology, Ulm University, Ulm D-89081, Germany
[9] Synchrotron SOLEIL, L'Orme de Merisiers, Saint Aubin-BP48, Gif-sur-Yvette CEDEX, France.
[10] CNRS, University of Bordeaux, UMS 3626 Placamat F-33608 Pessac, France
[11] INRA, UR629 Ecologie des Forêts Méditerranéennes (URFM), Avignon, France

*Corresponding author

Authors' contributions: S.D. and C.E.L.D. conceived the original screening and research plans (tomography); E.B., A.K., N.L., R.B., J.M.T.R., H.C., N.M-P, S.J., B.C. and S.D. performed the HRCT scans; G.C. and J.M.T.R. performed leaf hydraulics experiments; G.C. and J.C.D. performed gas exchange experiments. C.E.L.D. provided plant materials; G.C., G.A.G. and S.D. analyzed the data and wrote the article with contributions of all the authors.

One-sentence summary

Direct, non-invasive observations of embolism formation and repair reveal a lack of refilling under negative pressure and a xylem hydraulic vulnerability segmentation in grapevine.

Funding informations

This study has been carried out with financial support from the Cluster of Excellence COTE (ANR-10-LABX-45, within Water Stress and Vivaldi projects), and AgreenSkills Fellowship program, which has received funding from the EU's Seventh Framework Programme under grant agreement N° FP7 26719 (AgreenSkills contract 688). This work was also supported by the programme 'Investments for the Future' (ANR-10-EQPX-16, XYLOFOREST) from the French National Agency for Research. BC was supported by an Australian Research Council Future Fellowship (FT130101115) and travel funding provided by the International Synchrotron Access Program (ISAP) managed by the Australian Synchrotron.

Present address: UMR 1202 Biodiversité Gènes & Communautés INRA/Université Bordeaux, Bâtiment B2 - allée G. St Hilaire, CS 50023, 33615 Pessac Cedex – France

Phone: +33 5 40 00 36 64

e-mail: guillaume.charrier@bordeaux.inra.fr

Abstract

The vascular system of grapevine has been reported as being highly vulnerable, even though grapevine regularly experiences seasonal drought. Stomata would consequently remain open below water potentials that would generate a high loss of stem hydraulic conductivity via xylem embolism. This situation would necessitate daily cycles of embolism repair to restore hydraulic function.. However, a more parsimonious explanation is that some hydraulic techniques are prone to artifacts in species with long vessels, leading to overestimation of vulnerability. The aim of this study was to provide an unbiased assessment of (i) the vulnerability to drought-induced embolism in perennial and annual organs, and (ii) the ability to refill embolized vessels in two *Vitis* species.

X-ray micro-CT observations on intact plants indicated that both *V. vinifera* and *V. riparia* were relatively vulnerable, with the pressure inducing 50% loss of stem hydraulic conductivity (Ψ_{50Stem}) = -1.7 and -1.3MPa, respectively. In *V. vinifera*, both the stem and petiole had similar sigmoidal vulnerability curves, but differed in Ψ_{50} (-1.7 and -1.0 MPa for stem and petiole, respectively). Refilling was not observed as long as bulk xylem pressure

remained negative (*e.g.* at the apical part of the plants): P = -0.11 ± 0.02MPa; ΔPLC = 0.02 ± 0.01%. However, positive xylem pressure was observed at the basal part of the plant (P = 0.04 ± 0.01MPa), leading to recovered conductance (ΔPLC = -0.24 ± 0.12%).

Our findings provide evidence that grapevine is unable to repair embolized xylem vessels under negative pressure, but its hydraulic vulnerability segmentation provides a significant protection of the perennial stem.

Keywords: drought stress, stem, petiole, leaf, embolism resistance, hydraulic conductance, 3D imaging, *Vitis vinifera*.

Introduction

The plant hydraulic system is located at the interface between soil water and the atmosphere. Evaporative demand from the atmosphere generates a tension within a continuous xylem water column, pulling water from the soil, through roots, stems, petioles, and leaves (Dixon, 1896). Under drought conditions, the overall resistance to water flow through the soil-plant continuum increases. Increased resistance to water flow results from changes in the resistance at multiple specific locations along the flow pathway: in the soil, at the soil-root interface, in the roots, the main plant axis (*i.e.*, stems, branches), the petioles, and the leaves. Two primary mechanisms controlling the resistance are stomatal closure (leaf-to-air water flow) and the loss of xylem hydraulic conductivity (soil-to-leaf water flow; Cochard *et al.*, 2002). Stomatal closure is closely related to decreasing plant water status (Brodribb & Holbrook, 2003) and is often considered to be a protective mechanism against the loss of xylem hydraulic conductivity (Tyree & Sperry, 1988; Jones & Sutherland, 1991). Loss of xylem hydraulic conductivity occurs when the water potential of xylem sap reaches levels negative enough to disrupt the metastability of the water column, potentially resulting in embolism.

Generally, high resistance to embolism is observed in species distributed in dry environments, whereas highly vulnerable species are distributed in wet environments (Maherali *et al.*, 2004; Choat *et al.*, 2012). Although grapevine (*Vitis vinifera*) is widely cultivated, including in regions where it is frequently exposed to water deficit during the growing season (Lovisolo *et al.*, 2010), recent studies have produced contrasting estimates of its resistance to embolism. Grapevine has been described as either vulnerable (Zufferey *et al.*, 2011; Jacobsen & Pratt, 2012), or relatively resistant (Choat *et al.*, 2010; Brodersen *et al.*, 2013). In *Vitis* species, and *V. vinifera* especially, stomatal closure is typically observed for midday leaf water potentials (Ψ_{leaf}) < -1.5MPa (Schultz, 2003). Thus, according to some studies, significant losses in xylem hydraulic conductivity should be observed before stomatal closure (Ψ_{50} >-1.0MPa; Jacobsen & Pratt, 2012; Jacobsen *et al.*, 2015), implying that embolism would be commonplace.

Risk of hydraulic dysfunction is mitigated along the hydraulic pathway by hydraulic segmentation, *i.e.* more distal organs such as leaves and petioles will be at greater risk to embolism than more basal organs such as the trunk (Tyree and Zimmermann 2002; Choat *et al.*, 2005). This could promote hydraulic safety in larger, perennial organs, which represent a

greater investment of resources for the plant. Hydraulic segmentation may occur in two ways. During transpiration, the xylem pressure will always be greater in more distal parts of the pathway (leaves and petioles). All else being equal, this translates to a greater probability of embolism in distal organs. However, organs may also differ in their vulnerability to embolism, compensating or exacerbating the effects of differences in xylem pressure along the pathway. If leaves or petioles were more vulnerable to embolism than branches and the trunk, then they would be far more likely to suffer embolism during periods of water-stress. This would allow petioles, leaves (Nolf *et al.*, 2015), or even young branches (Rood *et al.*, 2000), to become embolized without significant impact on the trunk and larger branches. In grapevine, petioles have been described as extremely sensitive to cavitation (Ψ_{50} *ca.* -1.0 MPa; Zufferey *et al.*, 2011). However, the hydraulic methods employed in these previous studies have been shown to be prone to artifacts (Wheeler *et al.*, 2013; Torres-Ruiz *et al.*, 2015), necessitating the use of a non-invasive assessment of drought-induced embolism.

High-Resolution Computed Tomography (HRCT) produces three dimensional images of xylem tissue *in situ*, allowing for a non-invasive assessment of embolism resistance. This technique has provided robust results in various plant species with contrasting xylem anatomy (Charra-Vaskou *et al.*, 2012; 2016; Torres-Ruiz *et al.*, 2014; Dalla-Salda *et al.*, 2014; Bouche *et al.*, 2016; Cochard *et al.*, 2015; Knipfer *et al.*, 2015). Synchrotron-based tomography facilities allow the visualization of intact plants, offering a non-invasive, *in vivo* estimation of the loss of hydraulic conductivity within the xylem (Choat *et al.*, 2016). Moreover, the quality of the X-ray beam in the synchrotron facilities provides high resolution and signal to noise ratio, making image analysis simple and accurate.

If grapevine were as vulnerable to xylem embolism as suggested in some studies, refilling of embolized vessels would be expected to occur on a frequent (daily) basis in order to maintain hydraulic continuity (Sperry *et al.*, 1994; Cochard *et al.*, 2001; Charrier *et al.*, 2013). Various refilling mechanisms have been proposed to date, including positive root/stem pressure, and refilling while the xylem is under negative pressure via water droplet growth (Salleo *et al.*, 1996; Brodersen *et al.*, 2010; Knipfer *et al.*, 2016). Positive pressure in xylem sap can be related to mineral nutrition and soil temperature in autumn or spring (Ewers *et al.*, 2001), and to soluble carbohydrate transport into the vessel lumen during winter (Améglio *et al.,* 2001; Charrier *et al.*, 2013). Refilling under negative pressure is based on the hypothesis that embolized vessels are isolated from surrounding functional vessels, permitting positive pressures to develop and the embolism to dissolve (Salleo *et al.*, 1996; Tyree *et al.*, 1999).

147 This process has been related to the chemistry of conduit walls (Holbrook & Zwieniecki,
148 1999), the geometry of interconduit bordered pits (Zwieniecki & Holbrook, 2000), and
149 phloem unloading (Nardini *et al.*, 2011). While refilling via positive pressure has been
150 described frequently (Sperry *et al.* 1987; 1994; Hacke & Sauter 1996; Cochard *et al.*, 2001;
151 Améglio *et al.*, 2004; Cobb *et al.*, 2007), refilling under negative pressure remains
152 controversial (Cochard *et al.*, 2013; 2015). In grapevine particularly, imaging techniques have
153 provided evidence of refilling in embolized vessels (Brodersen *et al.*, 2010), but uncertainties
154 remain regarding the xylem water potential measurement at the position of the scan.
155 The goal of the current study was to provide a non-invasive assessment of (i) the
156 vulnerability to drought-induced embolism in two widespread grapevine species in perennial
157 (*Vitis vinifera* and *V. riparia*) and annual (*V. vinifera*) organs, and (ii) the ability to refill
158 embolized vessels under positive or negative pressure (*V. vinifera*). This approach would
159 indicate whether embolism formation and repair are likely to occur on a daily basis, and/or if
160 hydraulic segmentation could protect perennial organs from drought stress. Stems and petioles
161 from intact *V. vinifera* cv. Cabernet Sauvignon, and *V. riparia* plants were scanned using
162 Synchrotron-based HRCT, characterizing their vulnerability to embolism and quantifying
163 their ability to refill at different positions along the plant axis (base and apex) in relation with
164 bulk xylem pressure. These data were integrated with other non-invasive techniques assessing
165 leaf hydraulics and transpiration.

166 # Results

167 ## *HRCT imaging, and embolism vulnerability in* V. vinifera *and* V. riparia

168 Embolism in stems (*V. vinifera* and *V. riparia*) and petioles (*V. vinifera*) was
169 characterized by direct observation provided by HRCT images. Two dimensional, transverse
170 slices of xylem were extracted from a 3D volume for image analysis. Typical cross sections
171 were presented in Figure 1 for *V. vinifera*. Embolized (*i.e.* air-filled) vessels appear as black
172 spots (highlighted red in insets). Well-hydrated plants (Ψ_{Stem} > -0.5MPa) exhibited none or
173 very few air-filled vessels in stems and petioles (Figure 1A and D). For both organs, the
174 percent loss of conductivity (PLC) measured was lower than 5%. At further dehydration (*ca.* -
175 1.1MPa), only a few vessels became air-filled in stems generating 9% loss of hydraulic
176 conductance (Figure 1B), whereas half of the vessels were already embolized in petioles (PLC
177 = 46.2%; Figure 1E). A more negative water potential (Ψ_{Stem} = -1.7MPa) induced a

considerable increase in the number of air-filled vessels in both stems, and petioles, PLC reaching 50.5%, and 96.5%, respectively (Figure 1C and F).

HRCT imaging was used to establish stem vulnerability curves (*i.e.* variation in PLC as a function of xylem pressure). In *V. vinifera*, vulnerability curves of both organs exhibited a similar sigmoid shape with the air-entry point (Ψ_e) observed at -1.22, and -0.26MPa in stems and petioles, respectively (Figure 2; Table I). Water potential inducing 50% loss of hydraulic conductance differed between stems (Ψ_{50Stem} = -1.73MPa) and petioles ($\Psi_{50Petiole}$ = -0.98MPa). Thus, when the water potential reached stem Ψ_e, petioles had already lost 66% of their conductivity. Significant differences were observed between *Vitis* species (P = 0.002; Figure 3): *V. riparia* being more vulnerable than *V. vinifera* (Ψ_e: -0.70 *vs* -1.22MPa, and Ψ_{50Stem}: -1.29 *vs* -1.73MPa, for *V. riparia* and *V. vinifera*, respectively).

Integration with leaf hydraulic conductance and gas exchange in V. vinifera

Changes in leaf hydraulic conductance (noted K_{Leaf}, but including a part of the petiole) and transpiration were assessed and the data were integrated with those obtained from the HRCT analyses above. Loss of K_{Leaf} exhibited a similar pattern to loss of hydraulic conductance in petioles: $\Psi_{50Petiole}$ = -0.98MPa; Ψ_{50Leaf} = -1.08MPa (Table I), however with differences in the sensitivity (69 < slp < 129 %.MPa^{-1}). Apparent K_{leaf} (K_{Leaf_Ap}) was shifted compared to K_{Leaf} (similar sensitivity: 134 %.MPa^{-1}, higher Ψ_{50Leaf_Ap}: -0.46MPa). Parameters of all vulnerability curves were significantly different from 0 (P< 0.001; Table I).

Considering the stem to leaf gradient in water potential measured during the gas exchange experiment (*i.e.* when stomata remained open, and water potential gradient maintained; $\Psi_{Stem} = 0.866 * \Psi_{Leaf} + 0.083$; $R^2 = 0.870$), loss of hydraulic function across stems, petioles and leaves was calculated depending on Ψ_{Leaf} (Figure 4). The petiole and leaf were closely coordinated, with 50% loss of function at *ca.* -1.0MPa, whereas the stem remained almost non-embolized (PLC = 2.5%) at this water potential and transpiration was reduced (5.4%). At lower water potentials, almost complete hydraulic dysfunction in petioles ($PLC_{Petiole}$ = 88% at Ψ = -1.70MPa) was observed and the stem exhibited significant embolism (PLC_{Stem} = 32.2%). The margin between Ψ_{50Stem} and either $\Psi_{50Petiole}$ or Ψ_{50Leaf} was relatively narrow (0.65 to 0.75MPa). However, taking the gradient in Ψ from stem to leaf into account, the 'effective' safety margin was slightly greater (0.80 to 0.90MPa). Under well-watered conditions, with high VPD (approx. 2500Pa), leaf and stem water potentials reached -

0.62 +/- 0.03MPa and -0.39 +/- 0.03MPa (mean +/- SE, n = 36), for leaves and stems, respectively. Under the normal operating range of water potential, the amount of PLC in the stem and petiole would therefore be low (0 and 17%, respectively), while transpiration would be limited (K_{ap} = 42%).

Xylem refilling in V. vinifera

Re-watered plants were scanned either in the basal (1 cm above the grafting), or in the distal part (*ca.* 1m above soil). In the basal part, significant changes in the amount of air-filled vessels were observed over a 24 hours period, after the plant was re-watered. Most vessels were dark gray (*i.e.* air-filled) before re-watering (PLC = 86.8%; Figure 5D). After 7.5 hours, evidence of xylem refilling and an increase in the number of functional vessels was observed (Figure 5E), even though PLC was barely affected (PLC = 81.2%). After 15.5 hours, many additional vessels had refilled, decreasing the PLC to 57.4% (Figure 5F). In contrast, in the upper part of re-watered plants, even after more than 48 hours of re-watering, there was no significant change in PLC (Figure 5A-C), even though most living cells remained alive (Fig. S1). Refilling was not observed at the apex (ΔPLC = 0.02 ± 0.01%), regardless of the initial levels of embolism (13.7% < PLC < 92.4%).

Figure 6 thus depicts the changes in basal and apical portions of the same plant, where xylem refilling was observed at the base (ΔPLC = -15.5%), and, at the same moment, no significant change in PLC was observed in the upper part (ΔPLC = +5.7%). Pressure transducers indicated that bulk xylem pressure was positive at the base (Ψ_{Stem} = +0.023 MPa) and negative at the apex (Ψ_{Stem} = - 0.015 MPa). Although stem water potential quickly increased after re-watering, it does not completely equilibrate along the whole stem even after more than 80 hours (Fig. S2). Negative pressure was indeed measured at the apex (Ψ = -0.013MPa), whereas it was positive at the base of the same plant (Ψ_{Stem} = +0.033 MPa). Although not all plants exhibited individual vessels being refilled with sap or positive pressure, significant changes in theoretical hydraulic conductance were only observed when xylem pressures were positive (Fig. 7A). Differences in water potential (P = 0.011) and PLC (P = 0.006) were thus observed depending on the distance from the soil, among the 5 replicates (Fig. 7B).

Discussion

Despite the fact that *Vitis vinifera* can be adapted to environments experiencing seasonal drought, studies differ in estimates of its hydraulic vulnerability and its classification as drought sensitive (Wheeler *et al.*, 2005; Jacobsen & Pratt, 2012), or drought resistant (Choat *et al.*, 2010; Brodersen *et al.*, 2013). Discrepancies among studies most probably lie in methodological issues, especially considering that *Vitis vinifera* is a long-vesselled species (Cochard *et al.*, 2013; Rockwell *et al.*, 2014; Zhang *et al.*, 2014). Here, for the first time, a non-invasive estimation of complete vulnerability curves was obtained using direct observations on intact *Vitis* plants by HRCT. Our results demonstrate that *V. vinifera* stems are more resistant to xylem embolism than previously estimated by centrifugation technique, and can sustain water potential lower < -1MPa (Ψ_{50Stem} = -1.7MPa). Contrastingly, *V. riparia* originates from riparian habitats and exhibited higher drought sensitivity –(Ψ_{50Stem} = 1.3MPa). Our findings also show that petioles are more vulnerable to embolism than stems, providing evidence for hydraulic vulnerability segmentation in grapevine. Xylem conduits refilling was observed in the basal part of the plant, where positive bulk pressure was recorded (Figure 5D-F; Fig. 6), but not in the apical part, where bulk pressure remained negative under experimental conditions (Figure 5A-C; Fig. 6).

In view of the current debate on drought resistance of long-vesselled species (Sperry *et al.*, 2012; Sperry, 2013; Cochard & Delzon, 2013; Hacke *et al.*, 2015; Cochard *et al*, 2015), vulnerability curves imply that either embolism occurs under almost immediately negative water potentials of the xylem sap ('exponential' vulnerability curves), or that embolism does not take place until a threshold at a more negative water potential is reached ('sigmoidal vulnerability curves). According to Figure 1, no embolism was observed at high xylem water potentials (Ψ>-1.0MPa) in stems of intact *V. vinifera* plants, suggesting that all vessels can support some level of negative pressure. In stems, the number of embolized vessels only increased once the pressure reached values lower than -1.5 MPa, which is consistent with results observed using Magnetic Resonance Imaging (MRI, Choat *et al.*, 2010), and HRCT (Knipfer *et al.*, 2015). Non-functional vessels (*i.e.* those that remained full of sap on our final cut images), represented *ca.* 5% of the theoretical conductance and were not included in our vulnerability curve analyses.

The high image resolution (*ca.* 3µm per voxel) provided by HRCT allowed the computation of a theoretical conductivity according to the diameters of individual vessels via the Hagen-Poiseuille equation (Figure 2; 3). Therefore, the theoretical loss of conductance

271 could be quantified at various xylem water potentials (as in Brodersen *et al.*, 2013), whereas
272 previous studies qualitatively assessed PLC from the number of air- *vs* sap-filled vessels.
273 Combined with a high number of specimens at a wide range of water potentials, these results
274 provide, for the first time, a complete vulnerability curve on intact stems (Ψ_{50Stem} = -1.73MPa)
275 and petioles ($\Psi_{50Petiole}$ = -0.98MPa) of *V. vinifera*. The vulnerability curves obtained are in
276 agreement with the level of drought-induced embolism resistance observed for grapevine in
277 studies using non-invasive techniques: synchrotron-based HRCT (Brodersen *et al.*, 2013),
278 Acoustic Emission analysis (AE; Vergeynst *et al.*, 2015), and MRI (Choat *et al.*, 2010).
279 Although the source and signal interpretation qualitatively differ across non-invasive
280 techniques, numerous studies combining these techniques on various species measured similar
281 levels of embolism resistance (Choat *et al.*, 2010; 2015; Charra-Vaskou *et al.*, 2012; 2016;
282 Charrier *et al.,* 2014; Ponomarenko *et al.,* 2014; Torres-Ruiz *et al.,* 2014; Vergeynst *et al.*,
283 2015). However, the Ψ_{50} values observed in the current study are slightly less negative than
284 those reported previously, with non-invasive methods (-1.7 *vs ca.* -2.0 MPa). This may have
285 been due to differences in plant material. Ontogenic developmental stages of the plant might
286 explain this discrepancy, where the development of secondary xylem along the course of the
287 season would increase embolism resistance in grapevine (Choat *et al*., 2010). Our results
288 demonstrate genotypic differences on stem vulnerability curves between *Vitis* species (*V.*
289 *vinifera vs. V. riparia*; Figure 3) and are consistent with the higher drought-sensitivity of *V.*
290 *riparia* compared to *V. arizonica* and *V. champinii* (Knipfer *et al.*, 2015).

291 Petioles were more vulnerable to embolism than stems in *V. vinifera* cv Cabernet
292 Sauvignon (Figure 1; 2). Only a few studies have reported petiole vulnerability curves for
293 grapevine. Similar behavior is reported in other *Vitis vinifera* cultivars using flowmeter
294 (Zufferey *et al.*, 2011), pressure sleeve (Tombesi *et al.*, 2014), or MRI (Hochberg *et al.*,
295 2016). Loss of conductance in petioles (HRCT-based) and leaves (rehydration kinetic
296 method) as measured with different techniques are remarkably similar (Figure 4) even though
297 computations of hydraulic conductance from HRCT image data are only theoretical.
298 Considering an inaccuracy of 2 voxels per vessel, average vessel diameters exhibited *ca.* 11
299 and 19% deviation in stem and petiole, respectively. However, PLC were only slightly
300 affected (± 0.9% in stem and petiole). HRCT-based images evidenced that xylem embolism
301 limits conductance in petioles. However, the minimum water potential experienced by the
302 petiole might have been lower than measured despite bagging the petiole for three hours

before scanning it. This would have led to slightly over-estimated vulnerability curves, and would require additional observations using, for example, a small-sized psychrometer to monitor the petiole water potential during dehydration. In leaves, xylem embolism and extra-xylary (*e.g.* symplasmic) pathways both seem to contribute to the reduction of leaf hydraulic conductance (Kim & Steudle, 2007; Scoffoni *et al.*, 2014; Bouche *et al.*, 2016). These results question the validity of stem water potential measurement using bagged leaves for high level of stress (*e.g.* as presented on Fig. 6) *i.e.* when the leaf is hydraulically disconnected from the stem. Although embolism in petioles could represent a "hydraulic fuse" at the leaf level, under well-watered conditions, reduced transpiration (*ca.* 40%) substantially limits petiole embolism to less than 20%. In addition, the relatively young plant material used in this study (1 to 2 months old) is relatively vulnerable (Choat *et al.*, 2010), but typically would not experience substantial drought in springtime.

A gradient in water potential along the entire plant might prevent embolism from propagating from distal to proximal parts without considerable difference in an organs' embolism vulnerability *per se* (Fig. 6; Bouche *et al.*, 2016). However, major anatomical differences in secondary growth, pit anatomy, and cell wall composition could also explain the higher embolism resistance of lignified organs, presenting fewer nucleation points, and lower primary xylem/secondary xylem ratio (Choat *et al.*, 2005). Resistance to embolism is indeed tightly linked to xylem anatomy at the interspecific level (Lens *et al.,* 2011), air bubbles nucleating onto cell walls, and propagating through pores of pit membrane (Jansen *et al.*, 2009; Schenk *et al.*, 2015). Through the gradient in water potential and hydraulic vulnerability segmentation, leaves and petioles isolate perennial parts of the plant from more negative water potentials and hydraulic failure under water deficit in grapevine (as demonstrated in this study) and some tropical tree species (Nolf *et al.*, 2015).

This study provides new lines of evidence regarding the potential artefacts that lead to vulnerability curves with an 'exponential' shape. The ratio between vessel and sample length impairs hydraulic measurements in long-vesselled species (Ennajeh *et al.*, 2011; Martin-StPaul *et al.*, 2014; Torres-Ruiz *et al.*, 2014; Choat *et al.*, 2016), although this is disputed by other studies (Sperry *et al.*, 2012; Pratt *et al.*, 2015). Furthermore, the 'exponential' shaped vulnerability curves imply that a grapevine stem would be 50% embolized before its leaf and stomatal conductance decrease, which seems unlikely (Nardini & Salleo, 2000). Moreover, investing carbon into structures (*i.e.* conduit walls) that would lose their function so readily

seems unlikely, especially considering the functional importance of carbon in plant physiology (Mencuccini, 2003; McDowell, 2011; Sala *et al.*, 2012; Hartmann *et al.*, 2013; Charrier *et al.*, 2015; Hartmann, 2015). Finally, the minimal water potential experienced by a plant on a seasonal basis (Ψ_{min}) is generally less negative than its Ψ_{50} value (Choat *et al.*, 2012).

The current study does not support high vulnerability of grapevine stems (Jacobsen *et al.*, 2015). In the present study, drought-stressed *V. vinifera* plants (10% to 90% stem PLC) were able to refill embolized vessels at the stem bases, but not the upper, distal stem portions (Figure 5-6). When observed, embolism refilling was always associated with positive root pressure (Fig. 7), consistent with the results of Knipfer *et al.* (2015). In the upper part the xylem sap remained at negative pressure (Fig. S2) and showed no refilling, even though vessel associated cells remained alive (Fig. S1). Root pressure has been credited as a strategy to recover from winter embolism (Ewers *et al.*, 2001) and has been observed in various angiosperm dicot species, such as *Alnus sp* (Sperry *et al.*, 1994), *Betula sp* (Sperry, 1988), *Juglans sp* (Améglio *et al.*, 2002; Charrier *et al.*, 2013), *Vitis sp* (Hales, 1727; Sperry *et al.*, 1987), and some tropical and temperate vines and lianas (Ewers *et al.*, 1997; Cobb *et al.*, 2007). These studies suggest that particular species are able to actively refill their vessels by generation of positive pressure in the early Spring. In both this paper and in previous studies, HRCT-based observations of xylem refilling in grapevine reveal water droplets clinging on vessel walls, which then increase in volume towards the center of the conduit lumen (Brodersen *et al.*, 2013; Knipfer *et al.*, 2015; Fig. 5). This may suggest that apoplastic sap is pressurized before invading conduits' lumen. Recently, Knipfer *et al.* (2016) reported xylem refilling in the absence of a root system *i.e.* in 3-5 cm long excised stem segments connected to a 2-cm tube, filled with a solution at 0.2 kPa (corresponding to 2 cm column height). However, excised segments no longer exhibited tension nor pressure and slight hydrostatic pressure, when connecting the sample at both ends, which, combined with capillary forces, might have been sufficient to observe xylem refilling. In the present study, even xylem positive pressure may not successfully lead to xylem refilling in all cases. Xylem pressures of 0.02 to 0.05MPa magnitude were observed, which should correspond to a 2 to 5m high water column, while apical portion remained at a slightly negative potential (-0.02 to -0.1 MPa), without refilling observed at the apex (Fig. 7). Xylem pressure may have been dissipated along the plant stems, and/or gas did not dissolve into xylem sap, delaying the occurrence of

positive pressure at higher parts. Although xylem refilling was not observed at the apex during our experiment, it may have been occurred after a longer period. However, the occurrence of negative water potential after more than 3 days without active transpiration, suggests that this phenomenon is not routine for *Vitis vinifera*. It is important to consider that only bulk xylem pressures were assessed in the current study. There is a possibility that pressure gradients are not homogeneous across a portion of the stem, or even between vessels that lie in close proximity to each other. Currently, experimental approaches do not exist for assessing *in situ* pressures at this scale, but this difficulty needs to be acknowledged. Given that refilling is a phenomenon occurring at the level of an individual vessel, one would expect that it would be the local pressure gradient environment that would dictate whether or not refilling would occur, and not necessarily the bulk level property, nor living cells' activity.

Previous observations of refilling under negative pressure may have resulted from artifacts such as those documented by Wheeler *et al.* (2013). Cutting stems under water when sap is under negative pressure may induce the artificial formation of air bubbles, leading to an overestimation of embolism vulnerability (Torres-Ruiz *et al.*, 2015; Ogasa *et al.*, 2016; Umebayashi *et al.*, 2016). Therefore, normal diurnal fluctuation in xylem tension could produce artefactual PLC fluctuations in stems (Torres-Ruiz *et al.*, 2015) or petioles (Zufferey *et al.*, 2011). Equally, variation in tension along the plant axis could cause misleading interpretations of refilling under negative pressure if the leaves sampled for measuring stem water potential are not directly adjacent to the part of the stem being scanned and/or if leaves experienced levels of stress great enough to result in their hydraulic disconnection from the parent plant. We thus observed negative leaf water potential, although bulk xylem pressure was positive at the base (*e.g.* on Fig. 6). This point should be of particular concern in light of the high vulnerability of grapevine petioles characterized in this and other studies. Water potential measurements would therefore have to be performed on downward leaves located as close as possible to the position of the HRCT area scanned (but only for a moderate level of stress). Alternative methods could include cutting stem segments after equilibration to atmospheric pressure, or the use of stem psychrometers.

Conclusion

Stems of *V. vinifera* are more resistant to drought stress than those of *V. riparia*, and are not able to refill under negative bulk xylem pressure. The hydraulic segmentation

generated from stem to leaf is reinforced by vulnerability segmentation between perennial and annual parts, which prevents perennial parts from experiencing more severe losses in hydraulic function. The insights obtained here about the drought response of *Vitis* highlighted the limitations of current methods to assess *in situ* xylem sap water potential. These results will help to assess drought resistance of different grapevine genotypes, and to manage irrigation in the field, and should also be of significant interest for other economically important long-vesseled plants (*e.g. Quercus sp*, *Olea sp*, *Eucalyptus sp*).

Material and methods

Plant material

Two widespread grapevine species were measured: *Vitis vinifera*, which is cultivated for grape production, and *Vitis riparia*, which is commonly used as a rootstock. The domesticated grapevine species *V. vinifera* L originates from the Caucasian area (Zecca *et al.*, 2012), and has been cultivated worldwide. This species was compared with *V. riparia* Michx., a native American grape distributed in North America, which is known to be much more drought-sensitive than *V. vinifera* (Carbonneau, 1985). One-year old potted plants from *V. vinifera* cv Cabernet Sauvignon and *V. riparia* 'Gloire de Montpellier', both grafted on *V. riparia* 'Gloire de Montpellier' were grown in 7.5L pots filled with commercial potting soil for 2 months until they reach *ca.* 1m height and 1cm basal stem diameter (5 to 10 leaves). Different sets of plants (n = 5 to 10 plants per pool) were used for HRCT scans, leaf hydraulic conductance (K_{Leaf}), and gas exchange measurements (see below).

In the HRCT pool, 10 *V. vinifera* and 10 *V. riparia* plants were exposed to different levels of water stress for one to three weeks to cover a wide range of water potentials. In 2015, the plants were scanned at *ca.* 1m height, two to three times during the four days HRCT observations (Mid-April 2015). Among this pool, 3 *V. vinifera* plants were re-watered after scanning until the soil was water-saturated to measure their ability to recover from different level of initial embolism (50% < PLC < 90%) in upper part. Re-watered plants were stored in shaded conditions to prevent active transpiration and scanned every 6 hours for up to 48 hours, while stem water potential was regularly measured (see details below). An additional rewatering experiment was performed in May 2016, on 5 additional plants of the same age and morphology as in 2015, focusing on the difference between apex and base (right above

the rootstock). The K_{Leaf} measurements were carried out two months later (June 2015) on eight well-hydrated plants of *V. vinifera*, which were up-rooted prior to measurements to allow their progressive dehydration within a daily course. In the gas exchange pool, eight *V. vinifera* plants were exposed to different levels of water stress, but of lower intensity than the HRCT plants (pre-dawn water potentials > -1.2MPa).

High Resolution X-ray Computed Tomography

Synchrotron-based computed microtomography was used to visualize air- and sap-filled vessels in the main stem and petiole of *V. vinifera* cv. Cabernet Sauvignon, and the main stem of *V. riparia*. In April 2015, plants were brought to the HRCT beamline (PSICHE) at the SOLEIL synchrotron facility. This beamline has a large, empty rotary stage, which allowed us to scan plants at different heights (*e.g.* basal and upper portions). Three hours before each scan, one leaf, located 10mm above the scanned area, was wrapped in a plastic bag and covered with aluminium foil in order to provide accurate stem water potential values (Ψ_{Stem}). The water potential was then measured right before the scan with a Scholander pressure chamber (Precis 2000, Gradignan, France). At the height of the scan, one leaf was carefully attached to the stem using a piece of tape. The main stem and petiole were scanned simultaneously using a high flux (3.10^{11} photons.mm^{-2}) 25 keV monochromatic x-ray beam. The projections were recorded with an Hamamatsu Orca Flash sCMOS camera equipped with a 250 µm thick LuAG scintillator. The complete tomographic scan included 1,500 projections, 50 ms seconds each, for a 180° rotation. Thus, samples were exposed for 75 s to the x-ray beam. Tomographic reconstructions were performed using PyHST2 software (Mirone *et al.*, 2014) using the Paganin method (Paganin, 2006), resulting in 1536^3 32-bit volumic images. The final spatial resolution was 3^3 µm^3 per voxel. Complementary measurements to visualize embolized conduits in grapevine petioles and refilling at the stem base were undertaken at the Diamond Light Source (DLS) and Swiss Light Source (SLS) synchrotron facilities, where similar plant material and the same experimental setup were used. For details of the I12 beamline (DLS) and the TOMCAT X02DA beamline (SLS), please refer to Bouche *et al.* (2016) and Choat *et al.* (2016), respectively.

Measurement of xylem pressure/tension

During rewatering experiments, xylem water potential was measured using three different set-ups (Fig. S2). Two were dedicated to measure xylem negative pressure:

scholander pressure chamber (described above), and psychrometers (PSY-1, ICT international, Armidale, Australia). In 2015 experiment, xylem water potential was only measured using Scholander pressure chamber. In 2016, stem psychrometers were mounted on the stem of two different plants, 10 cm above grafting, before re-watering. A 5-cm long portion of the stem was wrapped in parafilm (Alcan, Montreal, Canada) to ensure psychrometer sealing, at 5 to 10 cm below the scanning area. About 2 cm^2 of bark (and parafilm) was removed and a psychrometer was attached with clamps. The third set-up was dedicated to measure positive xylem pressure. When a clear decrease in the amount of embolized conduits was observed at the base, the apex of the plant was cut and immediately connected to a pressure transducer probe (26PCFFA6D, Honeywell, Morristown, USA), using an adapter tube, filled with deionized and degassed water (Thitithanakul *et al.*, 2012). Data was recorded on a CR1000 logger (Campbell, Logan, USA) at a time interval of 30 seconds. Once the signal stabilized (*ca.* 15 min.), the base was cut and connected to the pressure transducer following the same procedure.

Image analysis and vulnerability curves

On transverse cross section taken from the center of the scanned volume, the diameter and area of each individual air- and sap-filled vessels (embolised and functional, respectively) were measured in stems and/or petioles of each species using ImageJ software (http://rsb.info.nih.gov/ij). Air-filled vessels were highly contrasted with surrounding tissues. Thus a binary image was generated and vessels were extracted according to their dimensions, discarding particles lower than 10μm^2 (*ca.* 4 pixels).

After synchrotron experiments, all stems and petiole samples were wrapped up in moist paper and plastic bags and brought to the PIAF-INRA laboratory (Clermont Ferrand, France). Samples were cut 2mm above the previously scanned area, and scanned again using HRCT (Nanotom 180 XS; GE, Wunstorf, Germany) as described in Cochard *et al.* (2015). Vessels where sap was under negative pressure (*i.e.* functional vessels) immediately filled with air (as observed in Torres-Ruiz *et al.*, 2015), whereas living vessels were not affected by cutting (*i.e.* cytoplasm was left intact in the individual vessel elements, see Jacobsen *et al.*, 2015). Filled vessels in these images, were typically located in the outermost part of the xylem tissue, and discarded in the subsequent analyses.

For each species and organ, the theoretical specific hydraulic conductivity of a whole cross section (K_H) was calculated from the Hagen-Poiseuille equation using the individual diameter of sap- and air-filled vessels as:

$$K_H = \sum \frac{\pi \cdot \emptyset^4}{128 \cdot \eta \cdot A_{Xyl}} \quad (1)$$

with K_H: specific theoretical hydraulic conductivity ($kg.m^{-1}.MPa^{-1}.s^{-1}$); $\emptyset$: mean feret diameter of vessels (m), η: viscosity of water (1.002 mPa.s at 20°C), and A_{Xyl}: xylem area of the cross section (m^2).

The theoretical loss of hydraulic conductivity (PLC) was calculated as:

$$PLC = 100 \cdot \frac{K_{HA}}{K_{HMax}} \quad (2)$$

with K_{HA} and K_{HMax} representing the theoretical hydraulic conductivities of air-filled vessels, in initial and cut cross sections, respectively.

Vulnerability curves (PLC as a function of water potential) were fitted using the nls function with R software (R Development Core Team, 2013), according to the following equation:

$$PLC = \frac{1}{1+e^{\frac{slp}{25}(\Psi - \Psi_{50})}} \quad (3)$$

with slp being the derivative at the inflexion point Ψ_{50Stem}.

The air entry point (Ψ_e) was estimated from eq. 3 as 50/slp +Ψ_{50Stem} (Domec and Gartner 2001).

Leaf hydraulic conductance

Loss of K_{Leaf} was measured by using the rehydration kinetic method (Brodribb and Holbrook, 2003; Charra-Vaskou *et al.*, 2011) on eight *V. vinifera* cv Cabernet Sauvignon plants (N = 4-5 measurements per plant). Conductance measurements were performed using plants at different levels of water stress. Two contiguous fully-expanded leaves were bagged in plastic bags with wet paper towels for one hour before taking a measurement in order to cease transpiration and equilibrate water potential within the leaf. Leaf water potential (Ψ_{Leaf}) was measured on one leaf using a Scholander pressure chamber (Precis 2000, Gradignan,

France), while K_{Leaf} was measured on the second one. The second leaf was excised and immediately connected, under water, to a flow-meter to measure K_{Leaf}. The flow-meter was composed of a pressure transducer (Omega Engineering Ltd, Manchester, UK) connected to a datalogger (USB-TC-AI, MCC, USA), which measures the water pressure drop between a calibrated capillary PEEK tube and the leaf. This pressure drop was then converted into a flow rate to calculate the leaf conductance as the ratio between the maximum flow rate recorded during rehydration and the leaf water potential. Specific leaf conductance (K_S) was subsequently calculated dividing the leaf conductance by leaf area, which was measured using a leaf area meter (WinFolia 2007b, Regent Inst., Quebec, Canada). Leaf vulnerability curve (percent loss in K_{Leaf} as a function of water potential) was fitted using the nls function with R software (R Development Core Team, 2013), according to the equation:

$$PLK_{Leaf} = \frac{1}{1+e^{\frac{slp}{25}\cdot(\Psi-\Psi_{50Leaf})}} \quad (4)$$

with slp being the derivative at the inflexion point Ψ_{50Leaf}.

Gas exchange

Pre-dawn water potential (Ψ_{pd}) was measured on one leaf per plant, close to the rootstock prior to any light exposure, on nine *V. vinifera* cv Cabernet Sauvignon plants exposed to different levels of water stress ($-0.05 < \Psi_{pd} < -2$ MPa). Plants were then exposed to outside ambient conditions from 8:00 *a.m.* until 14:00 *p.m.*, during a sunny day (PAR > 1500µmol.m^{-2}.s^{-1}; VPD > 2000Pa). Leaf gas exchange measurements were conducted on mature, well-exposed leaves using a portable open-system including an infrared gas analyzer (GFS 3000, Walz – Germany). Conditions in the cuvette (*i.e.* PAR, temperature, VPD, and CO_2) were set equal to environmental conditions. Leaf transpiration rate (E, mmol.m^{-2}.s^{-1}) was measured during the morning, from 8:00 until 14:00. Water potentials were measured on the leaf used for gas exchange (Ψ_{Leaf}), and on another one, wrapped for one hour in plastic bag covered with aluminium foil (Ψ_{Stem}), using a Scholander pressure chamber (Precis 2000, Gradignan, France). Apparent leaf hydraulic conductance (K_{Leaf_Ap}) was calculated as the ratio between E and $\Delta\Psi = \Psi_{Stem} - \Psi_{Leaf}$:

$$K_{leaf_{Ap}} = \frac{E}{\Delta\Psi} \quad (5)$$

A leaf vulnerability curve (percent loss in K_{Leaf_Ap} as a function of water potential) was fitted using the nls function with R software (R Development Core Team, 2013), according to the equation:

$$PLK_{Leaf\_Ap} = \frac{1}{1+e^{\frac{slp}{25}\cdot(\Psi-\Psi_{50Leaf\_Ap})}} \quad (6)$$

with slp being the derivative at the inflexion point Ψ_{50Leaf_Ap}.

FDA staining

Detection of viability of x-ray exposed xylem cells was performed using a 9.6-µm FDA (fluorescein-diacetate; Sigma-Aldrich, Milwaukee, WI) solution, in combination with fluorescence light microscopy. One plant was analysed ten days after first exposure to x rays. Stem slices were obtained from the exposed part and ten cm above this area. The stem was cut transversely, into 5mm thick slices, and immediately submerged into FDA solution for 30 minutes in the dark. Samples were rinsed with deionized water and placed onto a microscope glass slide. The sample surface was excited with green fluorescence light (λ = 490 nm) generated by a SOLA light engine SE 5-LCR-VB (Lumencor, Beaverton, USA), and observed for light λ > 500nm for detection of living and metabolically active tissue (green signal) using a macroscope Axiozoom V16 (Zeiss, Marly le Roy, France), connected to a camera Axiocam 105 (Zeiss, Marly le Roy, France).

Acknowledgments

This study has been carried out with financial support from the Cluster of Excellence COTE (ANR-10-LABX-45, within Water Stress and Vivaldi projects), and AgreenSkills Fellowship program, which has received funding from the EU's Seventh Framework Programme under grant agreement N° FP7 26719 (AgreenSkills contract 688). This work was supported by the programme 'Investments for the Future' (ANR-10-EQPX-16, XYLOFOREST) from the French National Agency for Research. The authors are also grateful to the PSICHE beamline (Soleil synchrotron facility, Gif-sur-Yvette, France), the TOMCAT beamline (Swiss Light Source, Paul Scherrer Institut, Villigen, Switzerland), and the I12 beamline (Diamond Light Source, United Kingdom). Vitality imaging was performed at the Bordeaux Imaging Center, which is a member of the national infrastructure France BioImaging, with the help of Brigitte Batailler.

Supplemental material

Supplementary figure S1 shows cell vitality at a distal part of grapevine stems, ten days after x-Ray exposure by HRCT scans.

Supplementary figure S2 illustrates the recovery in water potential measured via different methods *i.e.* stem psychrometer, pressure chamber and bagged leaf, and pressure transducer.

587 **Table I.** Details of the fit of different experimental data with a sigmoid function in *V. vinifera*.
588 Different techniques were used according to the studied organ: HRCT image analysis in stems
589 and petioles, measurement of rehydration kinetics at the leaf level and measurement of
590 transpiration loss depending on the water potential gradient from leaf to root. Degree of
591 freedom, residual sum of square and pseudo-R^2 are given. Values and significance of the two
592 parameters (Slope and Ψ_{50}) are indicated (***: $P<0.0001$), and Ψ_e calculated from these latter.

Organ	Technique	Df	SSres	Pseudo R^2	Slope (%.MPa^{-1})	Ψ_{50} (MPa)	Ψ_e (MPa)
Stem	HRCT	15	0.158	0.905	98.4***	-1.729***	-1.221
Petiole	HRCT	25	0.753	0.737	69.3***	-0.980***	-0.259
Leaf	Rehydration	32	0.207	0.948	129.0***	-1.084***	-0.696
Leaf	Transpiration	74	2.171	0.596	133.6***	-0.456***	-0.830

593

Figure caption

Figure 1. Transverse HRCT images of intact *Vitis vinifera* cv Cabernet Sauvignon plants at different water potentials: stems (A-C) and petioles (D-F). Insets represent 0.25 mm² area. Functional (grey) and air-filled (black) xylem vessels are represented in blue and red in the insets, respectively. Theoretical loss of hydraulic conductivity for each image is indicated as PLC (%). White bars = 1 mm.

Figure 2. Percentage loss of hydraulic conductivity (%) *versus* xylem water potential (MPa) calculated from HRCT images in *Vitis vinifera* stems (black dots) and petioles (grey dots). Dashed lines represent the sigmoid fit of the data. Symbols and bars represent the mean and standard errors from 0.2MPa classes (n= 1 to 7 replicates per dot).

Figure 3. Percentage loss of hydraulic conductivity (%) *versus* xylem water potential (MPa) calculated from HRCT images in stems of *Vitis vinifera* (black dots) and *Vitis riparia* (white dots). The dashed lines represent the sigmoid fit of the data (solid and dashed lines, for *V. vinifera* and *V. riparia*, respectively). Symbols and bars represent the mean and standard errors from 0.2MPa classes in *Vitis vinifera* (n= 1 to 7 replicates per dot), and *V. riparia* (1 replicate per dot).

Figure 4. Percentage loss of hydraulic conductivity (%) in *Vitis vinifera* stems (solid line; HRCT images), petioles (long-dashed line; HRCT images), leaves (short-dashed line; rehydration kinetic method), and apparent leaf conductance (dotted-line; calculated from gas exchange measurements) depending on leaf water potential (MPa).

Figure 5. Cross sections of *Vitis vinifera* stems at two different height levels *i.e.* the upper, distal part (A-C) and bottom, proximal part above the graft (D-F) after re-watering drought-stressed plants. Time relative to rewatering (t = 0 h, *i.e.* the rewatering time) and the theoretical losses of hydraulic conductance (PLC, %) are indicated. White bar = 1mm scale.

Figure 6. Cross section at two different height levels *i.e.* the upper, distal part (A-B) and bottom, proximal part above the graft (C-D) of the same *Vitis vinifera* plant, before and after re-watering. Time relative to rewatering (t = 0 h, *i.e.* the rewatering time), theoretical losses of hydraulic conductance (PLC), and water potential (MPa) measured using pressure chamber on bagged leaf (Ψ_{leaf}), stem psychrometer (Ψ_{stem}) and pressure probes (Ψ_{PP}) are indicated. White bar = 1mm scale. Discrepancy between Ψ_{leaf} and Ψ_{stem} probably originate from disconnection

624 from stem to leaf hydraulic pathway (according to Fig.4, when PLC_{apex} = 63%, Ψ_{leaf} = *ca.* -
625 2MPa and $PLC_{petiole}$ = *ca.* 100%).

626 **Figure 7.** Mean change in theoretical hydraulic conductance (-ΔPLC, %) and xylem water
627 potential (MPa) for basal and apical scan positions in re-watered stems of *Vitis vinifera*. PLC
628 and xylem water potential were significantly different across the apical and basal positions
629 based on a Kruskall-Wallis test (n = 5; *P* = 0.006 and 0.011, for PLC and water potential,
630 respectively).

631

632 **Figure S1.** Cross section of the upper stem part of a grapevine plant that was scanned with
633 HRCT 10 days before treatment with fluorescein-diacetate. The fluorescent, green colored
634 cells represent living cells, which were slightly more pronounced in the control image (B)
635 compared to the area that was exposed to the x-ray beam (A). White bar = 1mm scale.

636 **Figure S2.** A. Water potential (MPa) *versus* time relative to rewatering (t = 0 h, *i.e.* the
637 rewatering time) in re-watered *Vitis vinifera* plant. B. After significant change in theoretical
638 hydraulic conductance was observed (as shown Fig. 5), water potential was successively
639 measured on bagged leaf using pressure chamber (Ψ_{leaf}), then one pressure transducer was
640 connected to the apex (black line), and ultimately to the base (dotted line).

641

642 **References**

643 Ameglio T, Decourteix M, Alves G, Valentin V, Sakr S, Julien JL, Petel G, Guilliot A,
644 Lacointe A (2004) Temperature effects on xylem sap osmolarity in walnut trees: evidence
645 for a vitalistic model of winter embolism repair. Tree Physiology 24: 785-793.

646 Ameglio T, Bodet C, Lacointe A, Cochard H. (2002) Winter embolism, mechanisms of xylem
647 hydraulic conductivity recovery and springtime growth patterns in walnut and peach trees.
648 Tree Physiology 22: 1211-1220.

649 Ameglio T, Ewers FW, Cochard H, Martignac M, Vandame M, Bodet C, Cruiziat P (2001)
650 Winter stem xylem pressure in walnut trees: effects of carbohydrates, cooling and freezing.
651 Tree Physiology 21: 387-394.

652 Bouche PS, Delzon S, Choat B, Badel E, Brodribb TJ, Burlett R, Cochard H, Charra-Vaskou
653 K, Lavigne B, Li S, Mayr S, Morris H, Torres-Ruiz JM, Zufferey V, Jansen S (2016) Are
654 needles of *Pinus pinaster* more vulnerable to xylem embolism than branches? New insights
655 from X-ray computed tomography. Plant, Cell & Environment doi: 10.1111/pce.12680

Brodersen CR, McElrone AJ, Choat B, Lee EF, Shackel KA, Matthews MA (2013) In vivo visualizations of drought-induced embolism spread in *Vitis vinifera*. Plant Physiology 161: 1820-1829.

Brodersen CR, McElrone AJ, Choat B, Matthews MA, Shackel KA (2010) The dynamics of embolism repair in xylem: in vivo visualizations using high-resolution computed tomography. Plant Physiology 154: 1088-1095.

Brodribb TJ, Holbrook NM (2003) Stomatal closure during leaf dehydration, correlation with other leaf physiological traits. Plant Physiology 132: 2166-2173.

Carbonneau A (1985) The early selection of grapevine rootstocks for resistance to drought conditions. American Journal of Enology and Viticulture 36: 195–198.

Charra-Vaskou K, Badel E, Charrier G, Ponomarenko A, Bonhomme M, Foucat L, Mayr S, Améglio T (2016) Cavitation and water fluxes driven by ice water potential in *Juglans regia* during freeze–thaw cycles. Journal of Experimental Botany 67: 739-750.

Charra-Vaskou K, Badel E, Burlett R, Cochard H, Delzon S, Mayr S (2012) Hydraulic efficiency and safety of vascular and non-vascular components in *Pinus pinaster* leaves. Tree Physiology 32: 1161-1170.

Charra-Vaskou K, Mayr S (2011) The hydraulic conductivity of the xylem in conifer needles (*Picea abies* and *Pinus mugo*). Journal of Experimental Botany 62: 4383-4390.

Charrier G, Ngao J, Saudreau M, Améglio T (2015) Effects of environmental factors and management practices on microclimate, winter physiology, and frost resistance in trees. Frontiers in Plant Science, 6: 259.

Charrier G, Charra-Vaskou K, Kasuga J, Cochard H, Mayr S, Améglio T (2014) Freeze-thaw stress: effects of temperature on hydraulic conductivity and ultrasonic activity in ten woody angiosperms. Plant Physiology 164: 992–998.

Charrier G, Cochard H, Améglio T (2013) Evaluation of the impact of frost resistances on potential altitudinal limit of trees. Tree Physiology 33: 891–902.

Choat B, Badel E, Burlett R, Delzon S, Cochard H, Jansen S (2016) Non-invasive measurement of vulnerability to drought induced embolism by X-ray microtomography. Plant Physiology doi: 10.1104/pp.15.00732.

Choat B, Jansen S, Brodribb TJ *et al.* (2012) Global convergence in the vulnerability of forests to drought. Nature 491:752.

Choat B, Drayton WM, Brodersen C, Matthews MA, Shackel KA, Wada H, McElrone AJ (2010) Measurement of vulnerability to water stress-induced cavitation in grapevine: a comparison of four techniques applied to a longvesseled species. Plant, Cell & Environment 33: 1502–1512.

Choat B, Lahr EC, Melcher PJ, Zwieniecki MA, Holbrook NM (2005) The spatial pattern of air seeding thresholds in mature sugar maple trees. Plant, Cell & Environment 28: 1082-1089.

694 Cobb AR, Choat B, Holbrook NM (2007) Dynamics of freeze–thaw embolism in *Smilax*
695 *rotundifolia* (Smilacaceae). American Journal of Botany 94: 640-649.

696 Cochard H, Delzon S, Badel E (2015) X-ray microtomography (micro-CT): a reference
697 technology for high-resolution quantification of xylem embolism in trees. Plant, Cell &
698 Environment 38: 201-206.

699 Cochard H, Delzon S (2013) Hydraulic failure and repair are not routine in trees. Annals of
700 Forest Science 70: 659–661.

701 Cochard H, Badel E, Herbette S, Delzon S, Choat B, Jansen S (2013) Methods for measuring
702 plant vulnerability to cavitation: a critical review. Journal of Experimental Botany 64:
703 4779–4791.

704 Cochard H, Coll L, Le Roux X, Améglio T (2002) Unraveling the effects of plant hydraulics
705 on stomatal closure during water stress in walnut. Plant Physiology 128: 282-290.

706 Cochard H, Lemoine D, Ameglio T, Granier A (2001) Mechanisms of xylem recovery from
707 winter embolism in *Fagus sylvatica* L. Tree Physiology 21: 27-33.

708 Dalla-Salda G, Fernández ME, Sergent AS, Rozenberg P, Badel E, Martinez-Meier A (2014)
709 Dynamics of cavitation in a Douglas-fir tree-ring: transition-wood, the lord of the ring?
710 Journal of Plant Hydraulics 1: e-0005.

711 Dixon HH (1896) Transpiration into a saturated atmosphere. Proceedings of the Royal Irish
712 Academy.

713 Domec J-C, Gartner BL (2001) Cavitation and water storage capacity in bole xylem segments
714 of mature and young Douglas-fir trees. Trees 15: 204-214.

715 Ennajeh M, Simões F, Khemira H, Cochard H (2011) How reliable is the double-ended
716 pressure sleeve technique for assessing xylem vulnerability to cavitation in woody
717 angiosperms? Physiologia Plantarum 142: 205-210.

718 Ewers FW, Améglio T, Cochard H, Beaujard F, Martignac M, Vandame M, Bodet C, Cruiziat
719 P (2001) Seasonal variation in xylem pressure of walnut trees: root and stem pressures. Tree
720 Physiology 21: 1123-1132.

721 Ewers FW, Cochard H, Tyree MT (1997) A survey of root pressures in vines of a tropical
722 lowland forest. Oecologia 110: 191-196.

723 Hacke UG, Venturas MD, MacKinnon ED, Jacobsen AL, Sperry JS, Pratt RB. (2015) The
724 standard centrifuge method accurately measures vulnerability curves of long-vesselled olive
725 stems. New Phytologist 205: 116-127.

726 Hacke UG, Sperry JS (2003) Limits to xylem refilling under negative pressure in *Laurus*
727 *nobilis* and *Acer negundo.* Plant, Cell and Environment 26: 303–311.

728 Hacke UG, Sauter JJ (1996) Xylem dysfunction during winter and recovery of hydraulic
729 conductivity in diffuse-porous and ring-porous trees. Oecologia 105: 435-439.

730 Hales S (1727) Vegetable staticks, or an account of some statical experiments on the sap in
731 vegetables. J Peele, London.

732 Hartmann H, Ziegler W, Kolle O, Trumbore S (2013) Thirst beats hunger–declining
733 hydration during drought prevents carbon starvation in Norway spruce saplings. New
734 Phytologist 200: 340-349.

735 Hartmann H (2015) Carbon starvation during drought-induced tree mortality–are we chasing
736 a myth? Journal of Plant Hydraulics, 2, e005.

737 Hochberg U, Albuquerque C, Rachmilevitch S, Cochard H, David-Schwartz R, Brodersen
738 CR, McElrone A, Windt CW (2016) Grapevine petioles are more sensitive to drought
739 induced embolism than stems: evidence from in vivo MRI and microCT observations of
740 hydraulic vulnerability segmentation. Plant, Cell & Environment doi: 10.1111/pce.12688.

741 Holbrook NM, Zwieniecki MA (1999) Embolism repair and xylem tension: do we need a
742 miracle? Plant Physiology 120: 7-10.

743 Holbrook NM, Ahrens ET, Burns MJ Zwieniecki MA (2001). In vivo observation of
744 cavitation and embolism repair using magnetic resonance imaging. Plant Physiology 126:
745 27-31.

746 Jacobsen AL, Rodriguez-Zaccaro FD, Lee TF, Valdovinos J, Toschi HS, Martinez JA, Pratt
747 RB (2015) Grapevine xylem development, architecture and function. Functional and
748 Ecological Xylem Anatomy, 133-162.

749 Jacobsen AL, Pratt RB (2012) No evidence for an open vessel effect in centrifuge-based
750 vulnerability curves of a long-vesselled liana (*Vitis vinifera*). New Phytologist 194: 982-
751 990.

752 Jansen S, Choat B, Pletsers A (2009) Morphological variation of intervessel pit membranes
753 and implications to xylem function in angiosperms. American Journal of Botany 96: 409-
754 419.

755 Jones HG, Sutherland RA (1991) Stomatal control of xylem embolism. Plant, Cell &
756 Environment 14: 607-612.

757 Kim YX, Steudle E (2007) Light and turgor affect the water permeability (aquaporins) of
758 parenchyma cells in the midrib of leaves of *Zea mays*. Journal of Experimental Botany 58:
759 4119–4129.

760 Knipfer T, Eustis A, Brodersen CR, Walker AM, McElrone AJ (2015) Grapevine species
761 from varied native habitats exhibit differences in embolism formation/repair associated with
762 leaf gas exchange and root pressure. Plant, Cell & Environment 38: 1503–1513.

763 Knipfer T, Cuneo IF, Brodersen CR, McElrone AJ (2016) In situ visualization of the
764 dynamics in xylem embolism formation and removal in the absence of root pressure: a study
765 on excised grapevine stems. Plant physiology, 171: 1024-1036.

766 Lens F, Sperry JS, Christman MA, Choat B, Rabaey D, Jansen S (2011) Testing hypotheses
767 that link wood anatomy to cavitation resistance and hydraulic conductivity in the genus
768 *Acer*. New Phytologist 190: 709-723.

769 Lovisolo C, Perrone I, Carra A, Ferrandino A, Flexas J, Medrano H, Schubert A (2010)
770 Drought-induced changes in development and function of grapevine (*Vitis* spp.) organs and
771 in their hydraulic and non-hydraulic interactions at the whole-plant level: A physiological
772 and molecular update," Functional Plant Biology, 37: 98-116.

773 Maherali H, Pockman WT, Jackson RB (2004) Adaptive variation in the vulnerability of
774 woody plants to xylem cavitation. Ecology 85: 2184-2199.

775 Martin-St Paul NK, Longepierre D, Huc R, Delzon S, Burlett R, Joffre R, Rambal R, Cochard
776 H (2014) How reliable are methods to assess xylem vulnerability to cavitation? The issue of
777 'open vessel' artifact in oaks. Tree Physiology 34: 894-905.

778 McDowell NG (2011) Mechanisms linking drought, hydraulics, carbon metabolism, and
779 vegetation mortality. Plant Physiology 155: 1051-1059.

780 Mencuccini M (2003) The ecological significance of long-distance water transport: short-term
781 regulation, long-term acclimation and the hydraulic costs of stature across plant life forms.
782 Plant, Cell & Environment 26: 163- 182.

783 Mirone A, Brun E, Gouillart E, Tafforeau P, Kieffer J (2014) The PyHST2 hybrid distributed
784 code for high speed tomographic reconstruction with iterative reconstruction and a priori
785 knowledge capabilities, Nuclear Instruments and Methods in Physics Research Section B:
786 Beam Interactions with Materials and Atoms 324: 41-48.

787 Nardini A, Lo Gullo MA, Salleo S (2011) Refilling embolized xylem conduits: is it a matter
788 of phloem unloading? Plant Science 180: 604–611.

789 Nardini A, Salleo S (2000) Limitation of stomatal conductance by hydraulic traits: sensing or
790 preventing xylem cavitation? Trees 15: 14-24.

791 Nolf M, Creek D, Duursma R, Holtum J, Mayr S, Choat B (2015) Stem and leaf hydraulic
792 properties are finely coordinated in three tropical rainforest tree species. Plant, Cell &
793 Environment 38: 2652–2661.

794 Ogasa MY, Utsumi Y, Miki NH, Yazaki K, Fukuda K (2016) Cutting stems before relaxing
795 xylem tension induces artefacts in *Vitis coignetiae*, as evidenced by magnetic resonance
796 imaging. Plant, Cell & Environment 39: 329–337.

797 Paganin D, Mayo SC, Gureyev TE, Miller PR, Wilkins SW (2002) Simultaneous phase and
798 amplitude extraction from a single defocused image of a homogeneous object J. of
799 Microscopy 206:33-40.

800 Pratt RB, MacKinnon ED, Venturas MD, Crous CJ, Jacobsen AL (2015) Root resistance to
801 cavitation is accurately measured using a centrifuge technique. Tree Physiology 35: 185-
802 196.

803 Ponomarenko A, Vincent O, Pietriga A, Cochard H, Badel E, Marmottant P (2014) Ultrasonic
804 emissions reveal individual cavitation bubbles in water-stressed wood. Journal of the Royal
805 Society – Interface 11: 20140480.

806 R Development Core Team. (2015) R: A Language and Environment for Statistical
807 Computing, R Foundation for Statistical Computing, Vienna, Austria, https://www.R-
808 project.org.

809 Rockwell FE, Wheeler JK, Holbrook NM (2014) Cavitation and its discontents: opportunities
810 for resolving current controversies. Plant Physiology, 164: 1649-1660.

811 Rood SB, Patiño S, Coombs K, Tyree MT (2000) Branch sacrifice: cavitation-associated
812 drought adaptation of riparian cottonwoods. Trees 14: 248-257.

813 Sala A, Woodruff DR, Meinzer FC (2012) Carbon dynamics in trees: feast or famine? Tree
814 Physiology 32: 764-775.

815 Salleo S, Gullo MAL, Paoli D, Zippo M (1996) Xylem recovery from cavitation-induced
816 embolism in young plants of Laurus nobilis: a possible mechanism. New Phytologist 132:
817 47-56.

818 Schenk HJ, Steppe K, Jansen S (2015) Nanobubbles: a new paradigm for air-seeding in
819 xylem. *Trends in plant science*, *20*: 199-205.

820 Schultz HR (2003) Differences in hydraulic architecture account for near-isohydric and
821 anisohydric behaviour of two field-grown *Vitis vinifera* L. cultivars during drought. Plant,
822 Cell & Environment 26: 1393-1405.

823 Scoffoni C, Vuong C, Diep S, Cochard H, Sack L (2014) Leaf shrinkage with dehydration:
824 coordination with hydraulic vulnerability and drought tolerance. Plant Physiology 164:
825 1772–1788.

826 Sperry JS (2013) Cutting-edge research or cutting-edge artefact? An overdue control
827 experiment complicates the xylem refilling story. Plant, Cell & Environment 36: 1916-1918.

828 Sperry JS, Christman MA, Torres-Ruiz JM, Taneda H, Smith DD (2012) Vulnerability curves
829 by centrifugation: is there an open vessel artefact, and are'r' shaped curves necessarily
830 invalid? Plant, Cell & Environment 35: 601-610.

831 Sperry JS, Nichols KL, Sullivan JE, Eastlack SE (1994) Xylem embolism in ring-porous,
832 diffuse-porous, and coniferous trees of northern Utah and interior Alaska. Ecology 75:
833 1736-1752.

834 Sperry JS (1988) Winter xylem embolism and spring recovery in *Betula cordifolia*, *Fagus*
835 *grandifolia*, *Abies balsamea* and *Picea rubens*. Water Transport in Plants under Climatic
836 Stress. Cambridge University Press, Cambridge, UK, 86-98.

837 Sperry JS, Holbrook NM, Zimmermann MH, Tyree MT (1987) Spring filling of xylem
838 vessels in wild grapevine. Plant Physiology 83: 414-417.

839 Thitithanakul S, Pétel G, Chalot M, Beaujard F (2012) Supplying nitrate before bud break
840 induces pronounced changes in nitrogen nutrition and growth of young poplars. Functional
841 Plant Biology, 39: 795-803.

842 Tombesi S, Nardini A, Farinelli D, Palliotti A (2014) Relationships between stomatal
843 behavior, xylem vulnerability to cavitation and leaf water relations in two cultivars of *Vitis*
844 *vinifera*. Physiologia plantarum 152: 453-464.

845 Torres-Ruiz JM, Jansen S, Choat B, McElrone AJ, Cochard H, Brodribb TJ, Badel E, Burlett
846 R, Bouche PS, Brodersen CR, Li S, Morris H, Delzon S (2015) Direct X-ray
847 microtomography observation confirms the induction of embolism upon xylem cutting
848 under tension. Plant Physiology 167: 40-43.

849 Torres-Ruiz JM, Cochard H, Mayr S, Beikircher B, Diaz-Espejo A, Rodriguez-Dominguez
850 CM, Badel E, Fernández JE (2014) Vulnerability to cavitation in Olea europaea current-year
851 shoots: further evidence of an open-vessel artifact associated with centrifuge and air-
852 injection techniques. Physiologia Plantarum 152: 465-474.

853 Tyree MT, Zimmermann MH (2002) Xylem structure and the ascent of sap. In TE Timell, ed,
854 Springer Series in Wood Science, Springer Verlag, Berlin, pp 283

855 Tyree MT, Salleo S, Nardini A, Gullo MAL, Mosca R (1999) Refilling of embolized vessels
856 in young stems of laurel. Do we need a new paradigm? Plant Physiology 120: 11-22.

857 Tyree MT, Sperry JS (1988) Do woody plants operate near the point of catastrophic xylem
858 dysfunction caused by dynamic water stress? Answers from a model. Plant Physiology 88:
859 574-580.

860 Umebayashi T, Ogasa MY, Miki NH, Utsumi Y, Haishi T, Fukuda K. (2016) Freezing xylem
861 conduits with liquid nitrogen creates artifactual embolisms in water-stressed broadleaf trees.
862 Trees 30: 305-316.

863 Vergeynst LL, Dierick M, Bogaerts JA, Cnudde V, Steppe K (2015) Cavitation: a blessing in
864 disguise? New method to establish vulnerability curves and assess hydraulic capacitance of
865 woody tissues. Tree Physiology 35: 400-409.

866 Wheeler JK, Huggett BA, Tofte AN, Rockwell FE, Holbrook NM (2013) Cutting xylem
867 under tension or supersaturated with gas can generate PLC and the appearance of rapid
868 recovery from embolism. Plant, Cell & Environment 36: 1938–1949.

869 Wheeler JK, Sperry JS, Hacke UG, Hoang N (2005) Inter-vessel pitting and cavitation in
870 woody Rosaceae and other vesselled plants: a basis for a safety versus efficiency trade-off
871 in xylem transport. Plant, Cell & Environment 28: 800-812.

872 Zecca G, Abbott J, Sun WB, Spada A, Sala F, Grassi F (2012) The timing and the mode of
873 evolution of wild grapes (*Vitis*). Molecular Phylogenetics and Evolution 62: 736–747.

874 Zhang YJ, Holbrook NM (2014) The stability of xylem water under tension: a long, slow spin
875 proves illuminating. Plant, Cell & Environment 37: 2652-2653.

876 Zufferey V, Cochard H, Ameglio T, Spring JL, Viret O (2011) Diurnal cycles of embolism
877 formation and repair in petioles of grapevine (*Vitis vinifera* cv. Chasselas). Journal of
878 Experimental Botany 62: 3885-3894.

879 Zwieniecki MA, Holbrook NM (2000) Bordered pit structure and vessel wall surface
880 properties. Implications for embolism repair. Plant Physiology 123: 1015-1020.

881

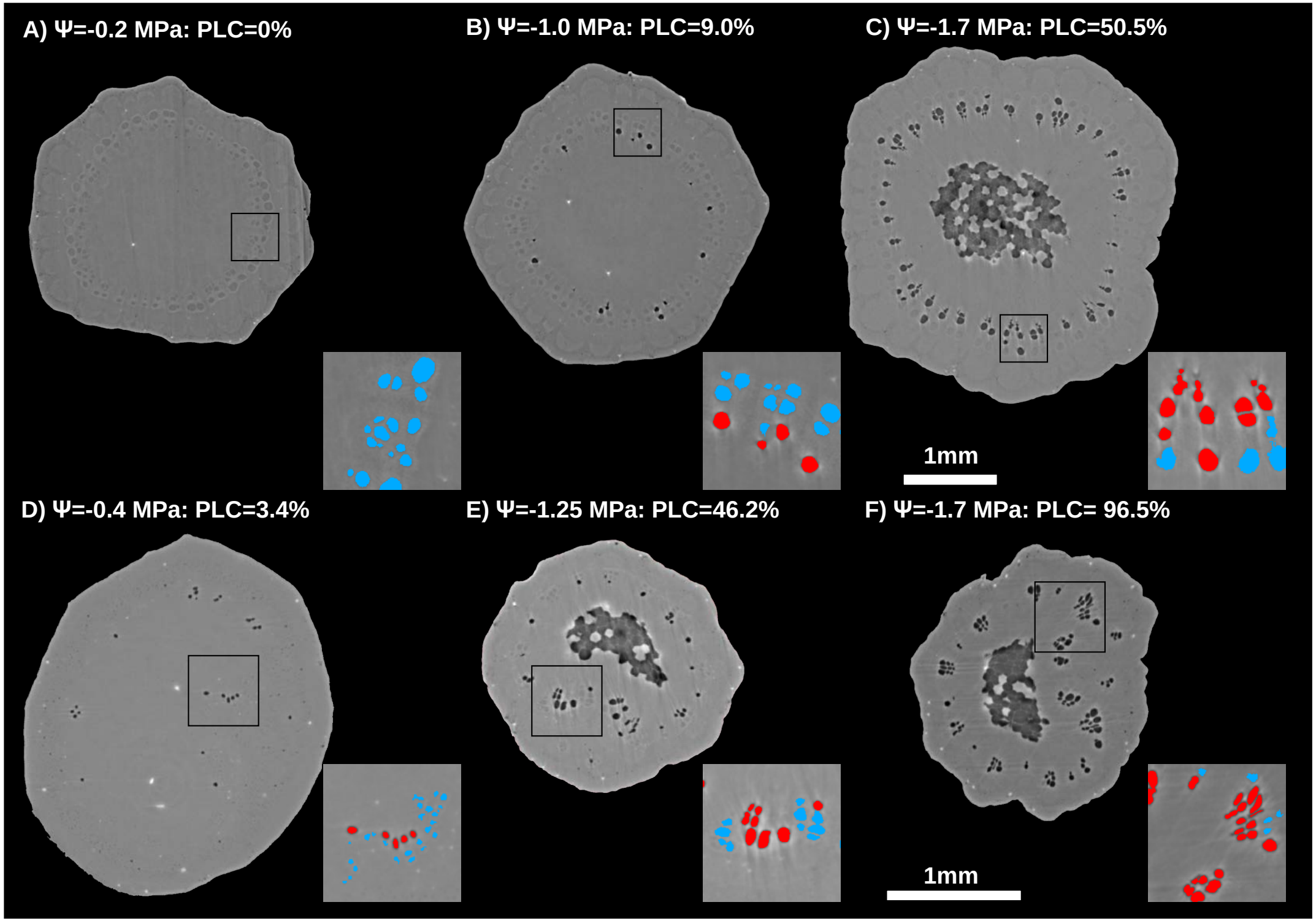

Figure 1. Transverse HRCT images of intact *Vitis vinifera* cv Cabernet-Sauvignon plants at different water potentials: stems (A-C) and petioles (D-F). Insets represent 0.25 mm² area. Functional (grey) and air-filled (black) xylem vessels are represented in blue and red spots in the insets, respectively. Theoretical loss of conductivity for each image is indicated as PLC (%). White bars = 1mm.

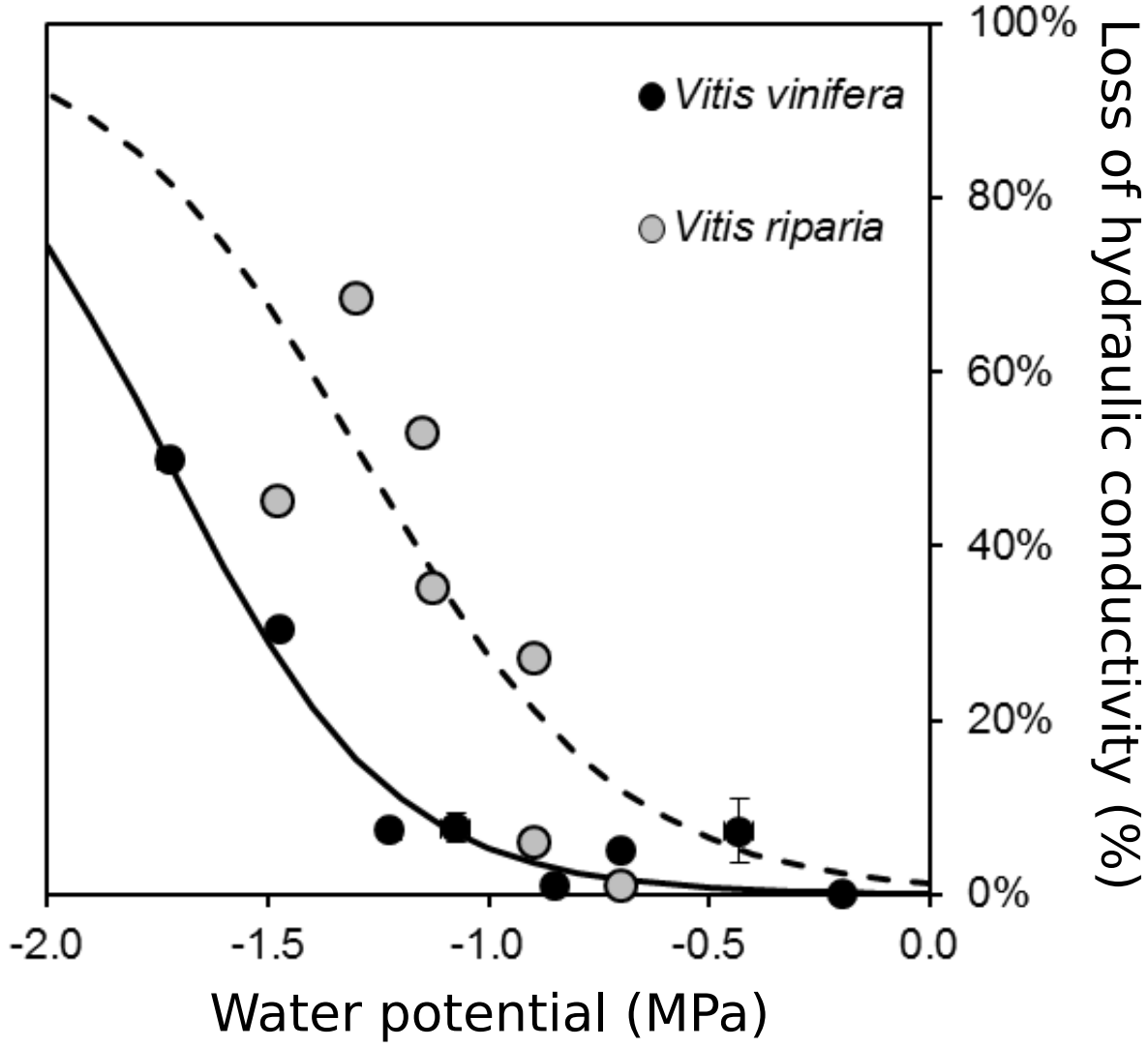

Figure 3. Percentage loss of conductivity (%) *versus* xylem water potential (MPa) calculated from HRCT images in stems of *Vitis vinifera* (black dots) and *Vitis riparia* (grey dots). The lines represent the sigmoid fit of the data (solid and dashed lines, for *V. vinifera* and *V. riparia*, respectively). Symbols and bars represent the mean and standard errors from 0.2MPa classes in *V. vinifera* (n= 1 to 7 replicates per dot), and *V. riparia* (1 replicate per dot).

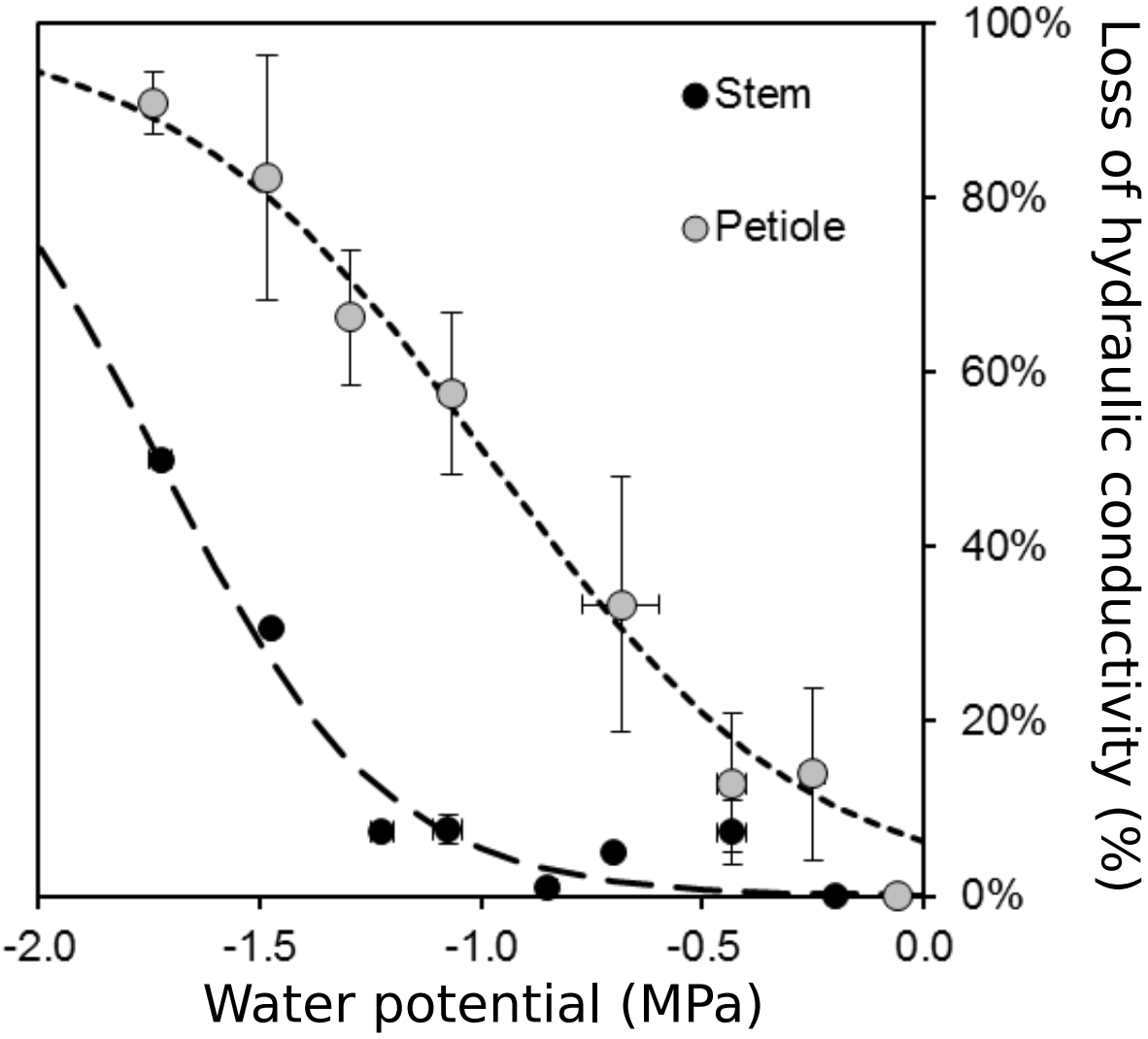

Figure 2. Percentage loss of conductivity (%) *versus* xylem water potential (MPa) calculated from HRCT images in *Vitis vinifera* stems (black dots) and petioles (grey dots). The dashed lines represent the sigmoid fit of the data. Symbols and bars represent the mean and standard errors from 0.2MPa classes (n= 1 to 7 replicates per dot).

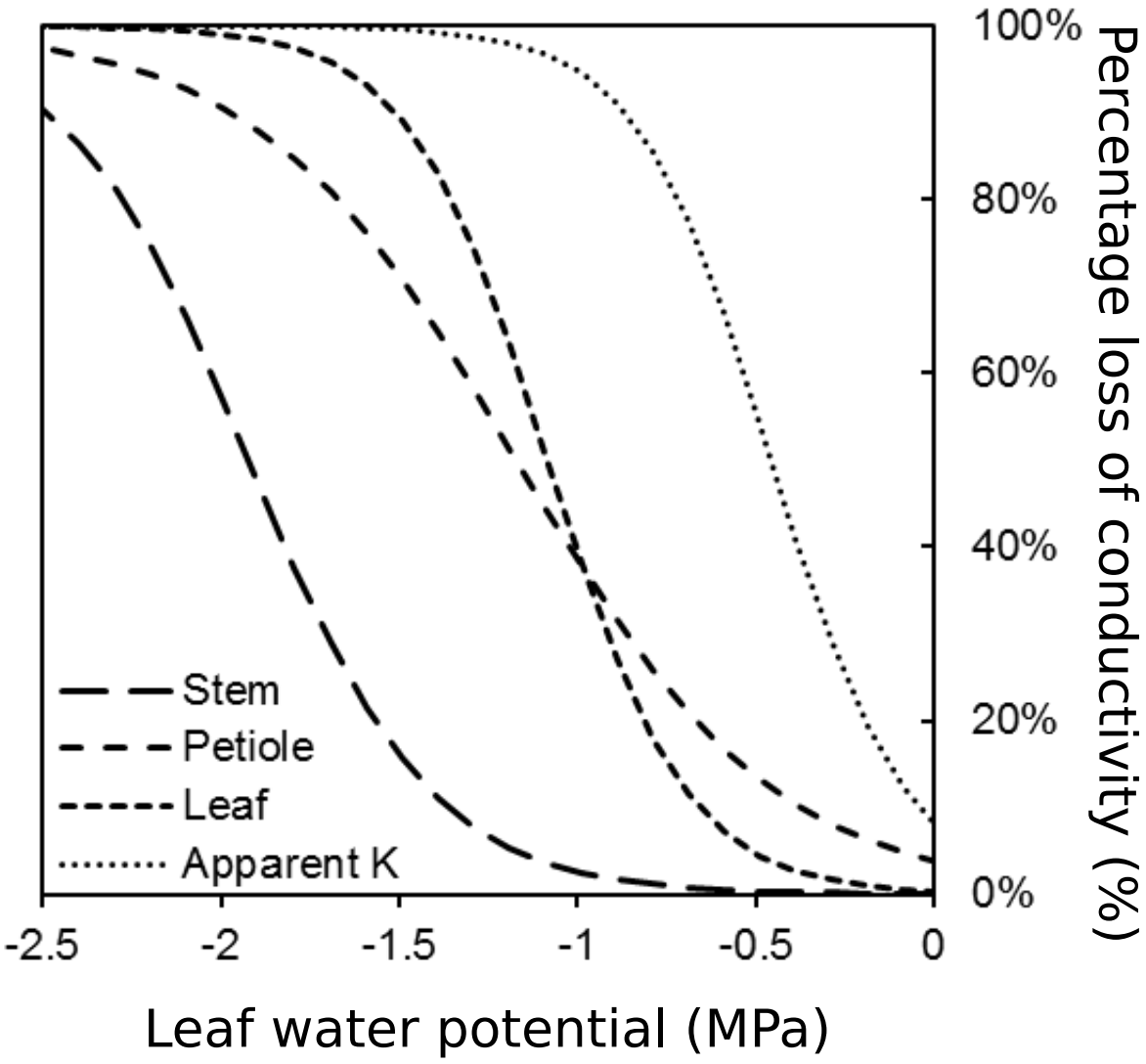

Figure 4. Percentage loss of conductivity (%) in *Vitis vinifera* stems (solid line; HRCT images), petioles (long-dashed line; HRCT images), leaves (short-dashed line; rehydration kinetic method), and apparent leaf conductance (dotted-line; calculated from gas exchange measurements) depending on leaf water potential (MPa).

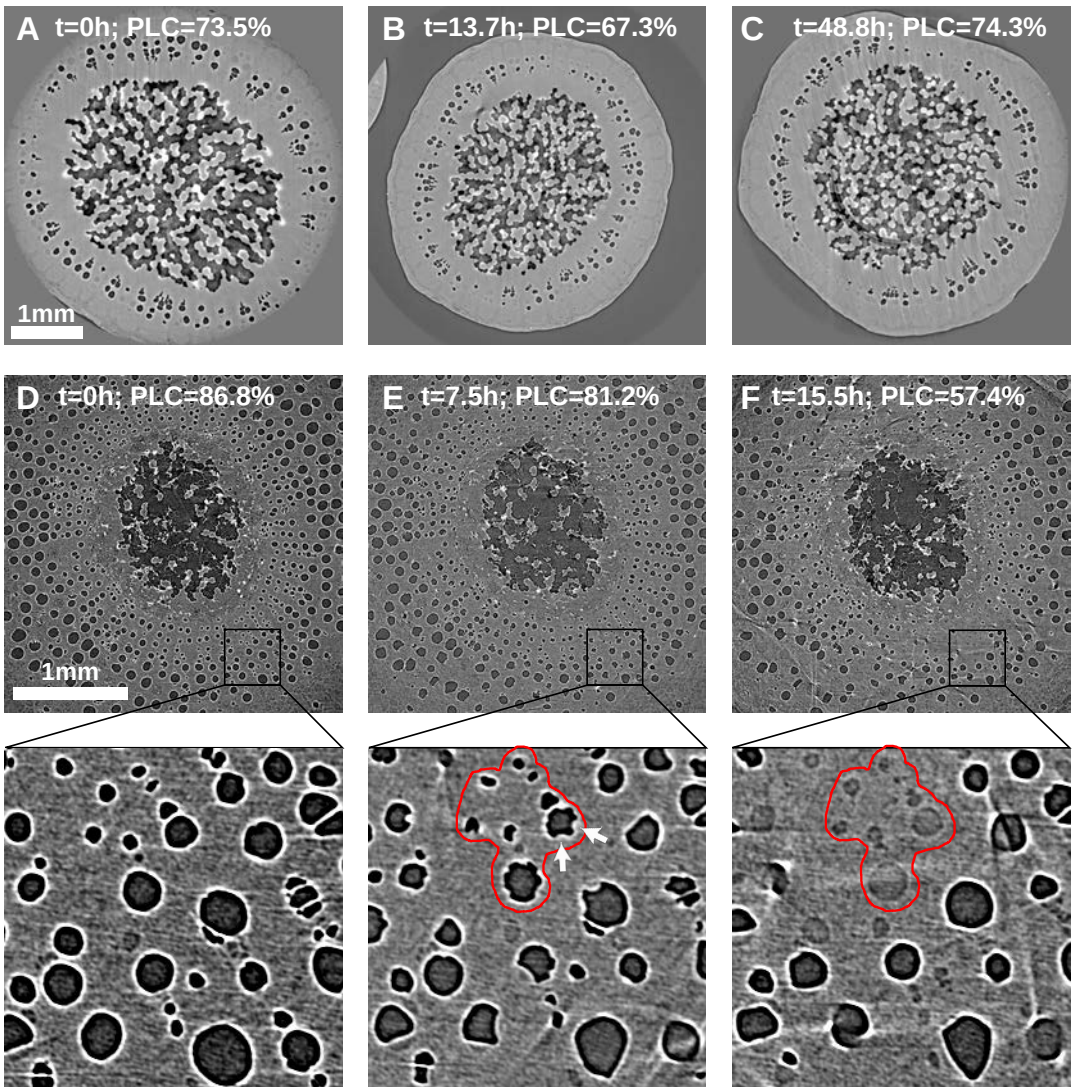

Figure 5. Cross section of *Vitis vinifera* stems at two different height levels *i.e.* the upper, distal part (A-C) and bottom, proximal part above the graft (D-F), after re-watering drought-stressed plants. Time relative to rewatering (t = 0 h, *i.e.* the rewatering time) and the theoretical losses of hydraulic conductance (PLC, %) are indicated. White bar = 1 mm scale.

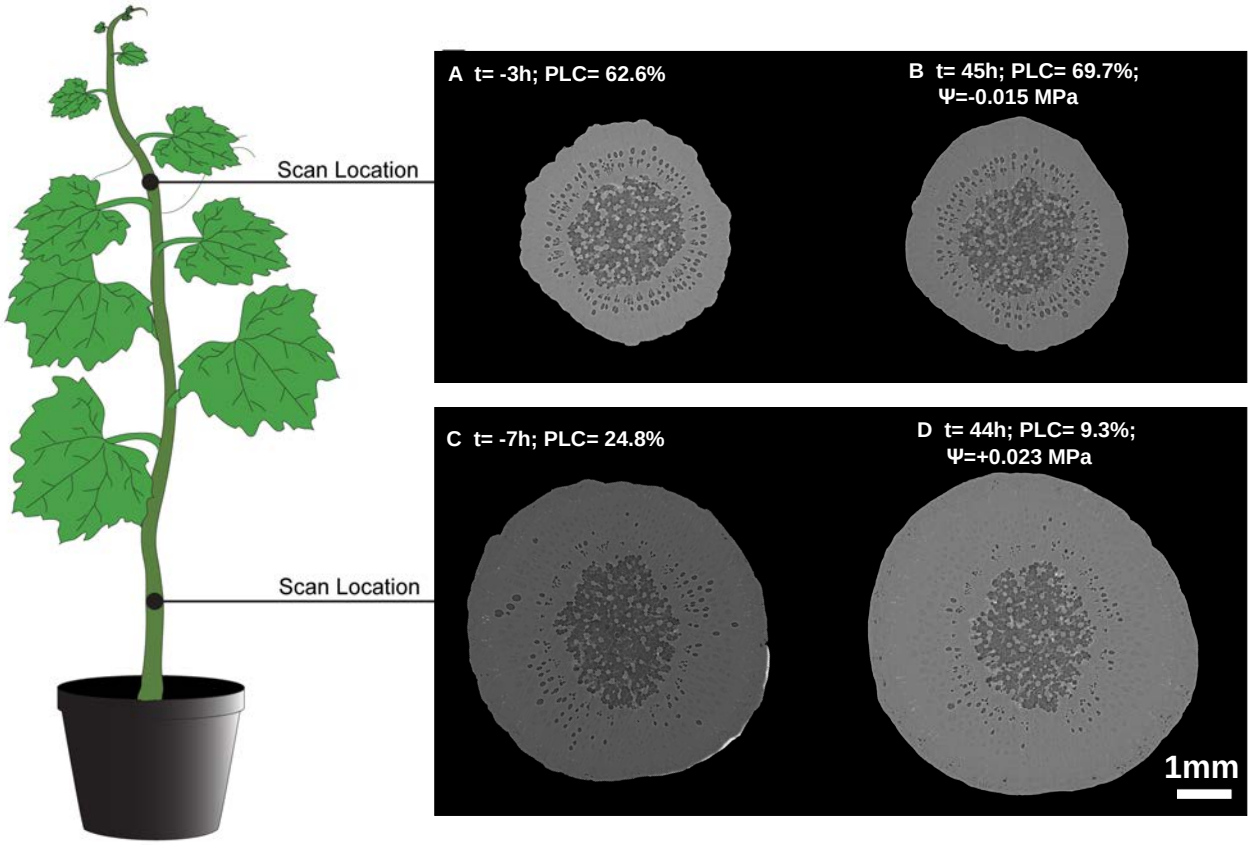

Figure 6. Cross section at two different height levels *i.e.* the upper, distal part (A-B) and bottom, proximal part above the graft (C-D) of the stem of the same *Vitis vinifera* plant, before and after rewatering. Time relative to rewatering (t = 0 h, *i.e.* the rewatering time), theoretical losses of hydraulic conductance (PLC, %), and water potential measured using pressure probes (Ψ, MPa) are indicated. White bar = 1mm scale.

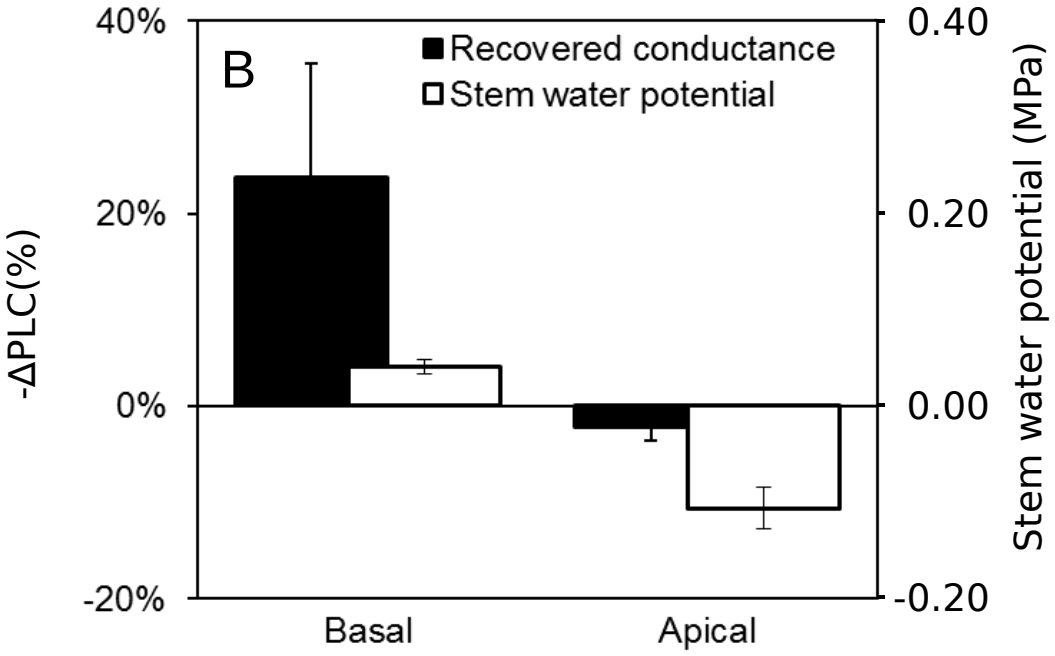

Figure 7. Mean change in theoretical hydraulic conductance (-ΔPLC, %) and xylem water potential (MPa) for basal and apical scan positions in re-watered stems of *Vitis vinifera*. PLC and xylem water potential were significantly different across the apical and basal positions based on a Kruskall-Wallis test (n = 5; P = 0.006, and 0.011, for PLC and water potential, respectively).

Parsed Citations

Ameglio T, Decourteix M, Alves G, Valentin V, Sakr S, Julien JL, Petel G, Guilliot A, Lacointe A (2004) Temperature effects on xylem sap osmolarity in walnut trees: evidence for a vitalistic model of winter embolism repair. Tree Physiology 24: 785-793.
Pubmed: Author and Title
CrossRef: Author and Title
Google Scholar: Author Only Title Only Author and Title

Ameglio T, Bodet C, Lacointe A, Cochard H. (2002) Winter embolism, mechanisms of xylem hydraulic conductivity recovery and springtime growth patterns in walnut and peach trees. Tree Physiology 22: 1211-1220.
Pubmed: Author and Title
CrossRef: Author and Title
Google Scholar: Author Only Title Only Author and Title

Ameglio T, Ewers FW, Cochard H, Martignac M, Vandame M, Bodet C, Cruiziat P (2001) Winter stem xylem pressure in walnut trees: effects of carbohydrates, cooling and freezing. Tree Physiology 21: 387-394.
Pubmed: Author and Title
CrossRef: Author and Title
Google Scholar: Author Only Title Only Author and Title

Bouche PS, Delzon S, Choat B, Badel E, Brodribb TJ, Burlett R, Cochard H, Charra-Vaskou K, Lavigne B, Li S, Mayr S, Morris H, Torres-Ruiz JM, Zufferey V, Jansen S (2016) Are needles of Pinus pinaster more vulnerable to xylem embolism than branches? New insights from X-ray computed tomography. Plant, Cell & Environment doi: 10.1111/pce.12680
Pubmed: Author and Title
CrossRef: Author and Title
Google Scholar: Author Only Title Only Author and Title

Brodersen CR, McElrone AJ, Choat B, Lee EF, Shackel KA, Matthews MA (2013) In vivo visualizations of drought-induced embolism spread in Vitis vinifera. Plant Physiology 161: 1820-1829.
Pubmed: Author and Title
CrossRef: Author and Title
Google Scholar: Author Only Title Only Author and Title

Brodersen CR, McElrone AJ, Choat B, Matthews MA, Shackel KA (2010) The dynamics of embolism repair in xylem: in vivo visualizations using high-resolution computed tomography. Plant Physiology 154: 1088-1095.
Pubmed: Author and Title
CrossRef: Author and Title
Google Scholar: Author Only Title Only Author and Title

Brodribb TJ, Holbrook NM (2003) Stomatal closure during leaf dehydration, correlation with other leaf physiological traits. Plant Physiology 132: 2166-2173.
Pubmed: Author and Title
CrossRef: Author and Title
Google Scholar: Author Only Title Only Author and Title

Carbonneau A (1985) The early selection of grapevine rootstocks for resistance to drought conditions. American Journal of Enology and Viticulture 36: 195-198.
Pubmed: Author and Title
CrossRef: Author and Title
Google Scholar: Author Only Title Only Author and Title

Charra-Vaskou K, Badel E, Charrier G, Ponomarenko A, Bonhomme M, Foucat L, Mayr S, Améglio T (2016) Cavitation and water fluxes driven by ice water potential in Juglans regia during freeze-thaw cycles. Journal of Experimental Botany 67: 739-750.
Pubmed: Author and Title
CrossRef: Author and Title
Google Scholar: Author Only Title Only Author and Title

Charra-Vaskou K, Badel E, Burlett R, Cochard H, Delzon S, Mayr S (2012) Hydraulic efficiency and safety of vascular and non-vascular components in Pinus pinaster leaves. Tree Physiology 32: 1161-1170.
Pubmed: Author and Title
CrossRef: Author and Title
Google Scholar: Author Only Title Only Author and Title

Charra-Vaskou K, Mayr S (2011) The hydraulic conductivity of the xylem in conifer needles (Picea abies and Pinus mugo). Journal of Experimental Botany 62: 4383-4390.
Pubmed: Author and Title
CrossRef: Author and Title
Google Scholar: Author Only Title Only Author and Title

Charrier G, Ngao J, Saudreau M, Améglio T (2015) Effects of environmental factors and management practices on microclimate, winter physiology, and frost resistance in trees. Frontiers in Plant Science, 6: 259.
Pubmed: Author and Title
CrossRef: Author and Title
Google Scholar: Author Only Title Only Author and Title

Charrier G, Charra-Vaskou K, Kasuga J, Cochard H, Mayr S, Améglio T (2014) Freeze-thaw stress: effects of temperature on hydraulic conductivity and ultrasonic activity in ten woody angiosperms. Plant Physiology 164: 992-998.
Pubmed: Author and Title
CrossRef: Author and Title

Google Scholar: Author Only Title Only Author and Title

Charrier G, Cochard H, Améglio T (2013) Evaluation of the impact of frost resistances on potential altitudinal limit of trees. Tree Physiology 33: 891-902.
Pubmed: Author and Title
CrossRef: Author and Title
Google Scholar: Author Only Title Only Author and Title

Choat B, Badel E, Burlett R, Delzon S, Cochard H, Jansen S (2016) Non-invasive measurement of vulnerability to drought induced embolism by X-ray microtomography. Plant Physiology doi: 10.1104/pp.15.00732.
Pubmed: Author and Title
CrossRef: Author and Title
Google Scholar: Author Only Title Only Author and Title

Choat B, Jansen S, Brodribb TJ et al. (2012) Global convergence in the vulnerability of forests to drought. Nature 491:752.
Pubmed: Author and Title
CrossRef: Author and Title
Google Scholar: Author Only Title Only Author and Title

Choat B, Drayton WM, Brodersen C, Matthews MA, Shackel KA, Wada H, McElrone AJ (2010) Measurement of vulnerability to water stress-induced cavitation in grapevine: a comparison of four techniques applied to a longvesseled species. Plant, Cell & Environment 33: 1502-1512.
Pubmed: Author and Title
CrossRef: Author and Title
Google Scholar: Author Only Title Only Author and Title

Choat B, Lahr EC, Melcher PJ, Zwieniecki MA, Holbrook NM (2005) The spatial pattern of air seeding thresholds in mature sugar maple trees. Plant, Cell & Environment 28: 1082-1089.
Pubmed: Author and Title
CrossRef: Author and Title
Google Scholar: Author Only Title Only Author and Title

Cobb AR, Choat B, Holbrook NM (2007) Dynamics of freeze-thaw embolism in Smilax rotundifolia (Smilacaceae). American Journal of Botany 94: 640-649.
Pubmed: Author and Title
CrossRef: Author and Title
Google Scholar: Author Only Title Only Author and Title

Cochard H, Delzon S, Badel E (2015) X-ray microtomography (micro-CT): a reference technology for high-resolution quantification of xylem embolism in trees. Plant, Cell & Environment 38: 201-206.
Pubmed: Author and Title
CrossRef: Author and Title
Google Scholar: Author Only Title Only Author and Title

Cochard H, Delzon S (2013) Hydraulic failure and repair are not routine in trees. Annals of Forest Science 70: 659-661.
Pubmed: Author and Title
CrossRef: Author and Title
Google Scholar: Author Only Title Only Author and Title

Cochard H, Badel E, Herbette S, Delzon S, Choat B, Jansen S (2013) Methods for measuring plant vulnerability to cavitation: a critical review. Journal of Experimental Botany 64: 4779-4791.
Pubmed: Author and Title
CrossRef: Author and Title
Google Scholar: Author Only Title Only Author and Title

Cochard H, Coll L, Le Roux X, Améglio T (2002) Unraveling the effects of plant hydraulics on stomatal closure during water stress in walnut. Plant Physiology 128: 282-290.
Pubmed: Author and Title
CrossRef: Author and Title
Google Scholar: Author Only Title Only Author and Title

Cochard H, Lemoine D, Ameglio T, Granier A (2001) Mechanisms of xylem recovery from winter embolism in Fagus sylvatica L. Tree Physiology 21: 27-33.
Pubmed: Author and Title
CrossRef: Author and Title
Google Scholar: Author Only Title Only Author and Title

Dalla-Salda G, Fernández ME, Sergent AS, Rozenberg P, Badel E, Martinez-Meier A (2014) Dynamics of cavitation in a Douglas-fir tree-ring: transition-wood, the lord of the ring? Journal of Plant Hydraulics 1: e-0005.
Pubmed: Author and Title
CrossRef: Author and Title
Google Scholar: Author Only Title Only Author and Title

Dixon HH (1896) Transpiration into a saturated atmosphere. Proceedings of the Royal Irish Academy.
Pubmed: Author and Title
CrossRef: Author and Title
Google Scholar: Author Only Title Only Author and Title

Domec J-C, Gartner BL (2001) Cavitation and water storage capacity in bole xylem segments of mature and young Douglas-fir trees. Trees 15: 204-214.
Pubmed: Author and Title

CrossRef: Author and Title
Google Scholar: Author Only Title Only Author and Title

Ennajeh M, Simões F, Khemira H, Cochard H (2011) How reliable is the double-ended pressure sleeve technique for assessing xylem vulnerability to cavitation in woody angiosperms? Physiologia Plantarum 142: 205-210.
Pubmed: Author and Title
CrossRef: Author and Title
Google Scholar: Author Only Title Only Author and Title

Ewers FW, Améglio T, Cochard H, Beaujard F, Martignac M, Vandame M, Bodet C, Cruiziat P (2001) Seasonal variation in xylem pressure of walnut trees: root and stem pressures. Tree Physiology 21: 1123-1132.
Pubmed: Author and Title
CrossRef: Author and Title
Google Scholar: Author Only Title Only Author and Title

Ewers FW, Cochard H, Tyree MT (1997) A survey of root pressures in vines of a tropical lowland forest. Oecologia 110: 191-196.
Pubmed: Author and Title
CrossRef: Author and Title
Google Scholar: Author Only Title Only Author and Title

Hacke UG, Venturas MD, MacKinnon ED, Jacobsen AL, Sperry JS, Pratt RB. (2015) The standard centrifuge method accurately measures vulnerability curves of long-vesselled olive stems. New Phytologist 205: 116-127.
Pubmed: Author and Title
CrossRef: Author and Title
Google Scholar: Author Only Title Only Author and Title

Hacke UG, Sperry JS (2003) Limits to xylem refilling under negative pressure in Laurus nobilis and Acer negundo. Plant, Cell and Environment 26: 303-311.
Pubmed: Author and Title
CrossRef: Author and Title
Google Scholar: Author Only Title Only Author and Title

Hacke UG, Sauter JJ (1996) Xylem dysfunction during winter and recovery of hydraulic conductivity in diffuse-porous and ring-porous trees. Oecologia 105: 435-439.
Pubmed: Author and Title
CrossRef: Author and Title
Google Scholar: Author Only Title Only Author and Title

Hales S (1727) Vegetable staticks, or an account of some statical experiments on the sap in vegetables. J Peele, London.
Pubmed: Author and Title
CrossRef: Author and Title
Google Scholar: Author Only Title Only Author and Title

Hartmann H, Ziegler W, Kolle O, Trumbore S (2013) Thirst beats hunger-declining hydration during drought prevents carbon starvation in Norway spruce saplings. New Phytologist 200: 340-349.
Pubmed: Author and Title
CrossRef: Author and Title
Google Scholar: Author Only Title Only Author and Title

Hartmann H (2015) Carbon starvation during drought-induced tree mortality-are we chasing a myth? Journal of Plant Hydraulics, 2, e005.
Pubmed: Author and Title
CrossRef: Author and Title
Google Scholar: Author Only Title Only Author and Title

Hochberg U, Albuquerque C, Rachmilevitch S, Cochard H, David-Schwartz R, Brodersen CR, McElrone A, Windt CW (2016) Grapevine petioles are more sensitive to drought induced embolism than stems: evidence from in vivo MRI and microCT observations of hydraulic vulnerability segmentation. Plant, Cell & Environment doi: 10.1111/pce.12688.
Pubmed: Author and Title
CrossRef: Author and Title
Google Scholar: Author Only Title Only Author and Title

Holbrook NM, Zwieniecki MA (1999) Embolism repair and xylem tension: do we need a miracle? Plant Physiology 120: 7-10.
Pubmed: Author and Title
CrossRef: Author and Title
Google Scholar: Author Only Title Only Author and Title

Holbrook NM, Ahrens ET, Burns MJ Zwieniecki MA (2001). In vivo observation of cavitation and embolism repair using magnetic resonance imaging. Plant Physiology 126: 27-31.
Pubmed: Author and Title
CrossRef: Author and Title
Google Scholar: Author Only Title Only Author and Title

Jacobsen AL, Rodriguez-Zaccaro FD, Lee TF, Valdovinos J, Toschi HS, Martinez JA, Pratt RB (2015) Grapevine xylem development, architecture and function. Functional and Ecological Xylem Anatomy, 133-162.
Pubmed: Author and Title
CrossRef: Author and Title
Google Scholar: Author Only Title Only Author and Title

Jacobsen AL, Pratt RB (2012) No evidence for an open vessel effect in centrifuge-based vulnerability curves of a long-vesselled liana (Vitis vinifera). New Phytologist 194: 982-990.

Pubmed: Author and Title
CrossRef: Author and Title
Google Scholar: Author Only Title Only Author and Title

Jansen S, Choat B, Pletsers A (2009) Morphological variation of intervessel pit membranes and implications to xylem function in angiosperms. American Journal of Botany 96: 409-419.
Pubmed: Author and Title
CrossRef: Author and Title
Google Scholar: Author Only Title Only Author and Title

Jones HG, Sutherland RA (1991) Stomatal control of xylem embolism. Plant, Cell & Environment 14: 607-612.
Pubmed: Author and Title
CrossRef: Author and Title
Google Scholar: Author Only Title Only Author and Title

Kim YX, Steudle E (2007) Light and turgor affect the water permeability (aquaporins) of parenchyma cells in the midrib of leaves of Zea mays. Journal of Experimental Botany 58: 4119-4129.
Pubmed: Author and Title
CrossRef: Author and Title
Google Scholar: Author Only Title Only Author and Title

Knipfer T, Eustis A, Brodersen CR, Walker AM, McElrone AJ (2015) Grapevine species from varied native habitats exhibit differences in embolism formation/repair associated with leaf gas exchange and root pressure. Plant, Cell & Environment 38: 1503-1513.
Pubmed: Author and Title
CrossRef: Author and Title
Google Scholar: Author Only Title Only Author and Title

Knipfer T, Cuneo IF, Brodersen CR, McElrone AJ (2016) In situ visualization of the dynamics in xylem embolism formation and removal in the absence of root pressure: a study on excised grapevine stems. Plant physiology, 171: 1024-1036.
Pubmed: Author and Title
CrossRef: Author and Title
Google Scholar: Author Only Title Only Author and Title

Lens F, Sperry JS, Christman MA, Choat B, Rabaey D, Jansen S (2011) Testing hypotheses that link wood anatomy to cavitation resistance and hydraulic conductivity in the genus Acer. New Phytologist 190: 709-723.
Pubmed: Author and Title
CrossRef: Author and Title
Google Scholar: Author Only Title Only Author and Title

Lovisolo C, Perrone I, Carra A, Ferrandino A, Flexas J, Medrano H, Schubert A (2010) Drought-induced changes in development and function of grapevine (Vitis spp.) organs and in their hydraulic and non-hydraulic interactions at the whole-plant level: A physiological and molecular update," Functional Plant Biology, 37: 98-116.
Pubmed: Author and Title
CrossRef: Author and Title
Google Scholar: Author Only Title Only Author and Title

Maherali H, Pockman WT, Jackson RB (2004) Adaptive variation in the vulnerability of woody plants to xylem cavitation. Ecology 85: 2184-2199.
Pubmed: Author and Title
CrossRef: Author and Title
Google Scholar: Author Only Title Only Author and Title

Martin-St Paul NK, Longepierre D, Huc R, Delzon S, Burlett R, Joffre R, Rambal R, Cochard H (2014) How reliable are methods to assess xylem vulnerability to cavitation? The issue of 'open vessel' artifact in oaks. Tree Physiology 34: 894-905.
Pubmed: Author and Title
CrossRef: Author and Title
Google Scholar: Author Only Title Only Author and Title

McDowell NG (2011) Mechanisms linking drought, hydraulics, carbon metabolism, and vegetation mortality. Plant Physiology 155: 1051-1059.
Pubmed: Author and Title
CrossRef: Author and Title
Google Scholar: Author Only Title Only Author and Title

Mencuccini M (2003) The ecological significance of long-distance water transport: short-term regulation, long-term acclimation and the hydraulic costs of stature across plant life forms. Plant, Cell & Environment 26: 163- 182.
Pubmed: Author and Title
CrossRef: Author and Title
Google Scholar: Author Only Title Only Author and Title

Mirone A, Brun E, Gouillart E, Tafforeau P, Kieffer J (2014) The PyHST2 hybrid distributed code for high speed tomographic reconstruction with iterative reconstruction and a priori knowledge capabilities, Nuclear Instruments and Methods in Physics Research Section B: Beam Interactions with Materials and Atoms 324: 41-48.
Pubmed: Author and Title
CrossRef: Author and Title
Google Scholar: Author Only Title Only Author and Title

Nardini A, Lo Gullo MA, Salleo S (2011) Refilling embolized xylem conduits: is it a matter of phloem unloading? Plant Science 180: 604-611.

Pubmed: Author and Title
CrossRef: Author and Title
Google Scholar: Author Only Title Only Author and Title

Nardini A, Salleo S (2000) Limitation of stomatal conductance by hydraulic traits: sensing or preventing xylem cavitation? Trees 15: 14-24.
Pubmed: Author and Title
CrossRef: Author and Title
Google Scholar: Author Only Title Only Author and Title

Nolf M, Creek D, Duursma R, Holtum J, Mayr S, Choat B (2015) Stem and leaf hydraulic properties are finely coordinated in three tropical rainforest tree species. Plant, Cell & Environment 38: 2652-2661.
Pubmed: Author and Title
CrossRef: Author and Title
Google Scholar: Author Only Title Only Author and Title

Ogasa MY, Utsumi Y, Miki NH, Yazaki K, Fukuda K (2016) Cutting stems before relaxing xylem tension induces artefacts in Vitis coignetiae, as evidenced by magnetic resonance imaging. Plant, Cell & Environment 39: 329-337.
Pubmed: Author and Title
CrossRef: Author and Title
Google Scholar: Author Only Title Only Author and Title

Paganin D, Mayo SC, Gureyev TE, Miller PR, Wilkins SW (2002) Simultaneous phase and amplitude extraction from a single defocused image of a homogeneous object J. of Microscopy 206:33-40.
Pubmed: Author and Title
CrossRef: Author and Title
Google Scholar: Author Only Title Only Author and Title

Pratt RB, MacKinnon ED, Venturas MD, Crous CJ, Jacobsen AL (2015) Root resistance to cavitation is accurately measured using a centrifuge technique. Tree Physiology 35: 185-196.
Pubmed: Author and Title
CrossRef: Author and Title
Google Scholar: Author Only Title Only Author and Title

Ponomarenko A, Vincent O, Pietriga A, Cochard H, Badel E, Marmottant P (2014) Ultrasonic emissions reveal individual cavitation bubbles in water-stressed wood. Journal of the Royal Society - Interface 11: 20140480.
Pubmed: Author and Title
CrossRef: Author and Title
Google Scholar: Author Only Title Only Author and Title

R Development Core Team. (2015) R: A Language and Environment for Statistical Computing, R Foundation for Statistical Computing, Vienna, Austria, https://www.R-project.org.

Rockwell FE, Wheeler JK, Holbrook NM (2014) Cavitation and its discontents: opportunities for resolving current controversies. Plant Physiology, 164: 1649-1660.
Pubmed: Author and Title
CrossRef: Author and Title
Google Scholar: Author Only Title Only Author and Title

Rood SB, Patiño S, Coombs K, Tyree MT (2000) Branch sacrifice: cavitation-associated drought adaptation of riparian cottonwoods. Trees 14: 248-257.
Pubmed: Author and Title
CrossRef: Author and Title
Google Scholar: Author Only Title Only Author and Title

Sala A, Woodruff DR, Meinzer FC (2012) Carbon dynamics in trees: feast or famine? Tree Physiology 32: 764-775.
Pubmed: Author and Title
CrossRef: Author and Title
Google Scholar: Author Only Title Only Author and Title

Salleo S, Gullo MAL, Paoli D, Zippo M (1996) Xylem recovery from cavitation-induced embolism in young plants of Laurus nobilis: a possible mechanism. New Phytologist 132: 47-56.
Pubmed: Author and Title
CrossRef: Author and Title
Google Scholar: Author Only Title Only Author and Title

Schenk HJ, Steppe K, Jansen S (2015) Nanobubbles: a new paradigm for air-seeding in xylem. Trends in plant science, 20: 199-205.
Pubmed: Author and Title
CrossRef: Author and Title
Google Scholar: Author Only Title Only Author and Title

Schultz HR (2003) Differences in hydraulic architecture account for near-isohydric and anisohydric behaviour of two field-grown Vitis vinifera L. cultivars during drought. Plant, Cell & Environment 26: 1393-1405.
Pubmed: Author and Title
CrossRef: Author and Title
Google Scholar: Author Only Title Only Author and Title

Scoffoni C, Vuong C, Diep S, Cochard H, Sack L (2014) Leaf shrinkage with dehydration: coordination with hydraulic vulnerability and drought tolerance. Plant Physiology 164: 1772-1788.
Pubmed: Author and Title
CrossRef: Author and Title

Google Scholar: Author Only Title Only Author and Title

Sperry JS (2013) Cutting-edge research or cutting-edge artefact? An overdue control experiment complicates the xylem refilling story. Plant, Cell & Environment 36: 1916-1918.
Pubmed: Author and Title
CrossRef: Author and Title
Google Scholar: Author Only Title Only Author and Title

Sperry JS, Christman MA, Torres-Ruiz JM, Taneda H, Smith DD (2012) Vulnerability curves by centrifugation: is there an open vessel artefact, and are'r' shaped curves necessarily invalid? Plant, Cell & Environment 35: 601-610.
Pubmed: Author and Title
CrossRef: Author and Title
Google Scholar: Author Only Title Only Author and Title

Sperry JS, Nichols KL, Sullivan JE, Eastlack SE (1994) Xylem embolism in ring-porous, diffuse-porous, and coniferous trees of northern Utah and interior Alaska. Ecology 75: 1736-1752.
Pubmed: Author and Title
CrossRef: Author and Title
Google Scholar: Author Only Title Only Author and Title

Sperry JS (1988) Winter xylem embolism and spring recovery in Betula cordifolia, Fagus grandifolia, Abies balsamea and Picea rubens. Water Transport in Plants under Climatic Stress. Cambridge University Press, Cambridge, UK, 86-98.
Pubmed: Author and Title
CrossRef: Author and Title
Google Scholar: Author Only Title Only Author and Title

Sperry JS, Holbrook NM, Zimmermann MH, Tyree MT (1987) Spring filling of xylem vessels in wild grapevine. Plant Physiology 83: 414-417.
Pubmed: Author and Title
CrossRef: Author and Title
Google Scholar: Author Only Title Only Author and Title

Thitithanakul S, Pétel G, Chalot M, Beaujard F (2012) Supplying nitrate before bud break induces pronounced changes in nitrogen nutrition and growth of young poplars. Functional Plant Biology, 39: 795-803.
Pubmed: Author and Title
CrossRef: Author and Title
Google Scholar: Author Only Title Only Author and Title

Tombesi S, Nardini A, Farinelli D, Palliotti A (2014) Relationships between stomatal behavior, xylem vulnerability to cavitation and leaf water relations in two cultivars of Vitis vinifera. Physiologia plantarum 152: 453-464.
Pubmed: Author and Title
CrossRef: Author and Title
Google Scholar: Author Only Title Only Author and Title

Torres-Ruiz JM, Jansen S, Choat B, McElrone AJ, Cochard H, Brodribb TJ, Badel E, Burlett R, Bouche PS, Brodersen CR, Li S, Morris H, Delzon S (2015) Direct X-ray microtomography observation confirms the induction of embolism upon xylem cutting under tension. Plant Physiology 167: 40-43.
Pubmed: Author and Title
CrossRef: Author and Title
Google Scholar: Author Only Title Only Author and Title

Torres-Ruiz JM, Cochard H, Mayr S, Beikircher B, Diaz-Espejo A, Rodriguez-Dominguez CM, Badel E, Fernández JE (2014) Vulnerability to cavitation in Olea europaea current-year shoots: further evidence of an open-vessel artifact associated with centrifuge and air-injection techniques. Physiologia Plantarum 152: 465-474.
Pubmed: Author and Title
CrossRef: Author and Title
Google Scholar: Author Only Title Only Author and Title

Tyree MT, Zimmermann MH (2002) Xylem structure and the ascent of sap. In TE Timell, ed, Springer Series in Wood Science, Springer Verlag, Berlin, pp 283
Pubmed: Author and Title
CrossRef: Author and Title
Google Scholar: Author Only Title Only Author and Title

Tyree MT, Salleo S, Nardini A, Gullo MAL, Mosca R (1999) Refilling of embolized vessels in young stems of laurel. Do we need a new paradigm? Plant Physiology 120: 11-22.
Pubmed: Author and Title
CrossRef: Author and Title
Google Scholar: Author Only Title Only Author and Title

Tyree MT, Sperry JS (1988) Do woody plants operate near the point of catastrophic xylem dysfunction caused by dynamic water stress? Answers from a model. Plant Physiology 88: 574-580.
Pubmed: Author and Title
CrossRef: Author and Title
Google Scholar: Author Only Title Only Author and Title

Umebayashi T, Ogasa MY, Miki NH, Utsumi Y, Haishi T, Fukuda K. (2016) Freezing xylem conduits with liquid nitrogen creates artifactual embolisms in water-stressed broadleaf trees. Trees 30: 305-316.
Pubmed: Author and Title
CrossRef: Author and Title

Google Scholar: Author Only Title Only Author and Title

Vergeynst LL, Dierick M, Bogaerts JA, Cnudde V, Steppe K (2015) Cavitation: a blessing in disguise? New method to establish vulnerability curves and assess hydraulic capacitance of woody tissues. Tree Physiology 35: 400-409.
Pubmed: Author and Title
CrossRef: Author and Title
Google Scholar: Author Only Title Only Author and Title

Wheeler JK, Huggett BA, Tofte AN, Rockwell FE, Holbrook NM (2013) Cutting xylem under tension or supersaturated with gas can generate PLC and the appearance of rapid recovery from embolism. Plant, Cell & Environment 36: 1938-1949.
Pubmed: Author and Title
CrossRef: Author and Title
Google Scholar: Author Only Title Only Author and Title

Wheeler JK, Sperry JS, Hacke UG, Hoang N (2005) Inter-vessel pitting and cavitation in woody Rosaceae and other vesselled plants: a basis for a safety versus efficiency trade-off in xylem transport. Plant, Cell & Environment 28: 800-812.
Pubmed: Author and Title
CrossRef: Author and Title
Google Scholar: Author Only Title Only Author and Title

Zecca G, Abbott J, Sun WB, Spada A, Sala F, Grassi F (2012) The timing and the mode of evolution of wild grapes (Vitis). Molecular Phylogenetics and Evolution 62: 736-747.
Pubmed: Author and Title
CrossRef: Author and Title
Google Scholar: Author Only Title Only Author and Title

Zhang YJ, Holbrook NM (2014) The stability of xylem water under tension: a long, slow spin proves illuminating. Plant, Cell & Environment 37: 2652-2653.
Pubmed: Author and Title
CrossRef: Author and Title
Google Scholar: Author Only Title Only Author and Title

Zufferey V, Cochard H, Ameglio T, Spring JL, Viret O (2011) Diurnal cycles of embolism formation and repair in petioles of grapevine (Vitis vinifera cv. Chasselas). Journal of Experimental Botany 62: 3885-3894.
Pubmed: Author and Title
CrossRef: Author and Title
Google Scholar: Author Only Title Only Author and Title

Zwieniecki MA, Holbrook NM (2000) Bordered pit structure and vessel wall surface properties. Implications for embolism repair. Plant Physiology 123: 1015-1020.
Pubmed: Author and Title
CrossRef: Author and Title
Google Scholar: Author Only Title Only Author and Title

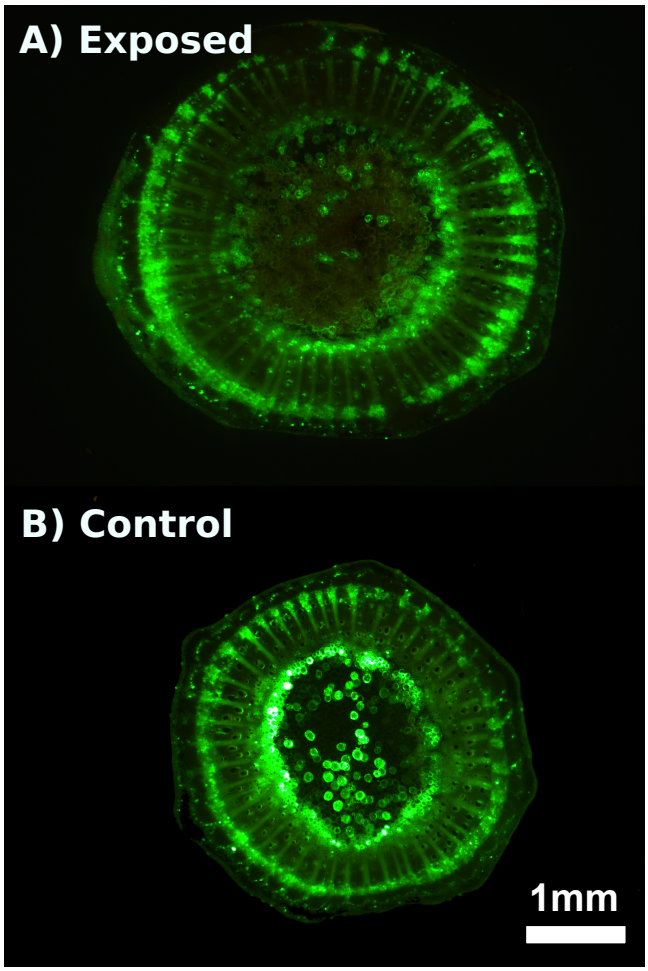

Figure S1. Cross section of the upper stem part of a grapevine plant that was scanned with HRCT 10 days before treatment with fluorescein-diacetate The fluorescent, green colored cells represent living cells, which were slightly more pronounced in the control image (B) compared to the area that was exposed to x-ray beam (A). White bar = 1mm scale.

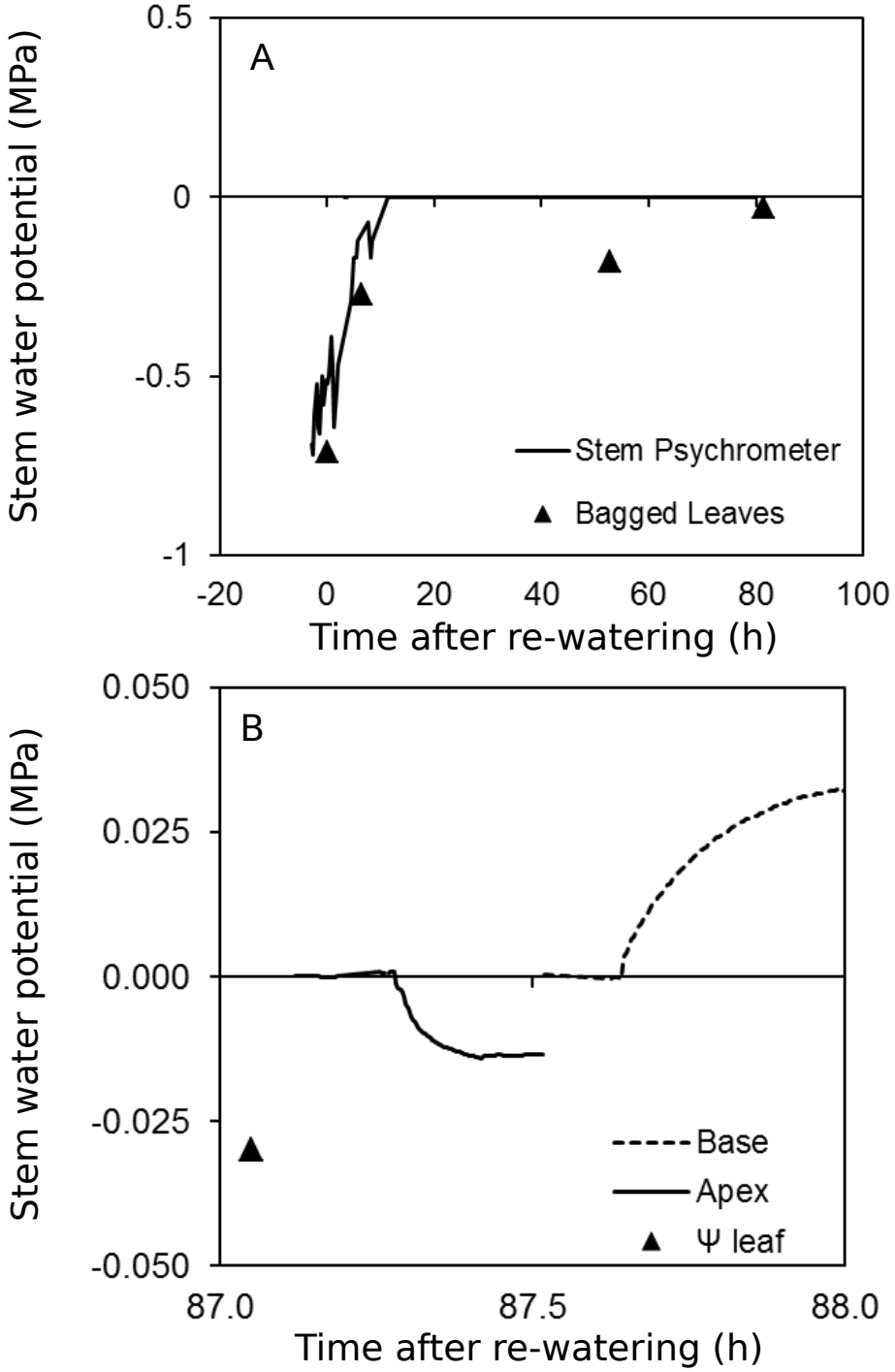

Figure S2. Water potential (MPa) *versus* time relative to re-watering (t = 0 h, *i.e.* the rewatering time) in re-watered *Vitis vinifera* plant, measured by stem psychrometer (A) and bagged leaf using pressure chamber (Ψ_{leaf}, A and B). **B.** After final scan, water potential was slightly negative on bagged leaf using pressure chamber (Ψ_{leaf}), and at the apex (*via* pressure transducer, black line), and positive at the base (dotted line).